COVID-19: Attacks the 1-Beta Chain of Hemoglobin and Captures the Porphyrin to Inhibit Human Heme Metabolism

Wenzhong Liu [1,2,*], Hualan Li[2]

[1] School of Computer Science and Engineering, Sichuan University of Science & Engineering, Zigong, 643002, China;
[2] School of Life Science and Food Engineering, Yibin University, Yibin, 644000, China;
[*]Correspondence.Wenzhong Liu, liuwz@suse.edu.cn.

Abstract

The novel coronavirus pneumonia is a contagious acute respiratory disease caused by the SARS-COV-2 coronavirus. The pathogenic mechanism of the novel coronavirus is unknown, which presents a significant impediment to the patient rescue. A conserved domain search strategy was utilized in this work to determine that a large number of viral proteins could bind to hemoglobin. S could bind to extracellular hemoglobin. SARS-COV-2 virus proteins interacted with porphyrins. SARS-COV-2 viruses could synthesize heme from porphobilinogen and encode all the similar enzymes required for the process. Both E and ORF3a contained heme-binding sites. ORF3a's Arg134 and E's Cys44 were the heme-iron binding sites, respectively. ORF3a also contained homologous domains to human cytochrome C reductase and bacterial EFeB protein. The molecular docking analysis revealed that ORF3a and ORF8 proteins were shown to be capable of attacking hemoglobin's 1-beta chain, whereas ORF3a was found to be effective in capturing heme for dissociation to iron and porphyrin. Deoxyhemoglobin was more susceptible to viral attack than oxidized hemoglobin. In summary, the combination of viral proteins to porphyrins and their metal compounds would improve the ability to permeate cell membranes and generate oxygen free radicals (ROS). It may be associated with viral infections and epidemic transmission. Viral proteins regulated the production and function of NO, CO and CO_2 by inhibiting the activity of hemoglobin, thereby affecting immune cell function. Viral proteins' attack on hemoglobin could result in symptoms such as respiratory distress and blood clotting, damage to numerous organs and tissues, and disruption of normal human heme metabolism.

Keywords: Novel Coronavirus; ORF3a; Respiratory distress; Blood; Coagulation; Cytokine Storm.

1. Background

The novel coronavirus pneumonia (COVID-19) is a contagious acute respiratory infectious disease. Patients with this disease show a fever over 37.3℃, with symptoms such as dry cough, fatigue and difficulty breathing, and frost-glass-like symptoms in the lungs(1-3). Some patients also have severe diarrhea(4), such as watery stools. Most mild patients get a better prognosis, butfor some serious patients, acute respiratory distress syndrome, shock, acidosis and coagulopathy quickly appear, and they even die. A lot of mucus, fibrin, and thrombosis are discovered in the dissected lung tissue(5, 6). The disease is highly transmitted. The current COVID-19 epidemic has shown the trend of a global pandemic at the beginning of the 21st

century.

Researchers performed virus isolation tests and nucleic acid sequencing to confirm that a novel coronavirus caused the disease(7, 8). It is noted that the nucleic acid of the novel coronavirus is a kind of positive-stranded RNA(8). Its structural proteins include: Spike Protein (S), envelope protein (E), membrane protein (M), and nucleocapsid phosphoprotein. Transcribed non-structural proteins consist of orf1ab, ORF3a, ORF6, ORF7a, ORF10 and ORF8. The novel coronavirusis highly homologous to the coronavirus in bats(9, 10), and has significant homology with the SARS virus(11, 12). Researchers have studied the function of novel coronavirus structural proteins and some non-structural proteins(13, 14). However, the novel coronavirus has potential genomic characteristics, some of which are the main cause of human outbreaks(15, 16). For example, the CoV EIC (Coronavirusenvelope protein ion channel) has been implicated in modulating virion release and CoV – host interaction(17). Spike proteins, ORF8 and ORF3a proteins are significantly different from other known SARS-like coronaviruses, and they may bring about more serious pathogenicity and transmission differences when compared with SARS-CoV(18). From earlier studies, it was found that the novel coronavirus enters epithelial cells through the spike protein interacting with the human ACE2 receptor protein on the surface, thus causing human infection. Due to the limitations of existing experimental methods, the specific functions of proteins such as ORF8 and ORF3a are still unclear. The pathogenicity mechanism of the novel coronavirus remains mysterious(19).

Literature(20) revealed biochemical examination indexes of 99 patients with the novel coronavirus pneumonia, and also reflected the abnormal phenomenon of hemoglobin-related biochemical indexes of patients. Besides, it was demonstrated that the hemoglobin and neutrophil counts of most patients decreased, and the index values of serum ferritin, erythrocyte sedimentation rate, C-reactive protein, albumin, and lactate dehydrogenase of many patients increased significantly. This trace implied that patients' hemoglobin was decreasing, and the body would accumulate too many harmful iron ions, which would form inflammation in the body and increase C-reactive protein and albumin. Cells react to stress due to inflammation, thus producing large amounts of serum ferritin to bind free iron ions to reduce damage. Hemoglobin's activity regulates the generation and function of gaseous molecules NO, CO, and CO2. Thereby it influences the phenotype of M1 and M2 macrophages and thus the TH1 and TH2 immune cytokine spectrum (21). Most carbon dioxide is transported in the form of bicarbonate in plasma, while a small portion of carbon dioxide is done by carbamoyl hemoglobin of erythrocytes. Oxygen is transported in the blood by hemoglobin of red blood cells. Hemoglobin is composed of four subunits, 2-α and 2-β, and each subunit has an iron-bound heme(22, 23). The heme is an essential component of hemoglobin. It is a porphyrin containing iron. The structure without iron is called porphyrins. When iron is divalent, hemoglobin can release carbon dioxide and capture oxygen atoms in alveolar cells, and iron is oxidized to the trivalent state. When hemoglobin is made available to other cells in the body through the blood, it can release oxygen atoms and capture carbon dioxide, and iron is reduced to the divalent state. Therefore, here it is thought that viral proteins may attack hemoglobin, causing the heme to dissociate into iron and porphyrins, and then the viral proteins capture the porphyrin. This interpretation was also consistent with some existing clinical features.

Both lungs hold the role of exchanging carbon dioxide and oxygen. The COVID-19 virus that attacked hemoglobin would yield iron, carbon dioxide, and oxygen, which might put both lung

cells in a toxic and inflammatory state. Then, it will form multiple ground glass images and penetration shadows on both sides of the lung(24-26), when ground glass images are often associated with rapid and noticeable hypoxemia.

In the early and severe stage, patients have varying degrees of respiratory distress symptoms. Many doctors have found that ECMO patients have some strange clinical features that are low oxygen, low blood oxygen saturation(27, 28) and high dissolved oxygen, which may be a critical reason in the low success rate of rescuing critical patients(29). ECMO is featured with cardiopulmonary function in vitro, and can help patients exchange oxygen and carbon dioxide in vitro. During this process, drugs such as the anticoagulant can be added at the same time. In this article, it is believed that this phenomenon indicates hemoglobin, which can carry oxygen in the blood of critically ill patients, became extremely low. Due to the deep attack of the virus, there is little normal functioning hemoglobin that can carry oxygen in the blood. Therefore, patients with ECMO have low oxygenation. If the virus can bind a large number of porphyrins, heme synthesis is inhibited. In this case, there is less hemoglobin synthesis. Besides, the virus attacks hemoglobin, which reduces the amount of hemoglobin that is typically oxygenated. Much hemoglobin can not carry oxygen after the attack. As a result, blood oxygen saturation decreases. Oxygenated hemoglobin is red blood cell hemoglobin that binds oxygen. After the virus attacks the oxidized hemoglobin, the lost oxygen atoms accumulate in the blood. As they hardly enter into the tissue cells, the dissolved oxygen in the blood gets higher.

Virus attacks will causedamage to many organs and tissues. For example, capillaries are easily broken due to inflammation(30). Proteins such as fibrinogen fill the capillaries' cracks through the coagulation reaction. Therefore, a lot of fibrin and thrombi accumulate in the lung tissue of critically ill patients(31). If the amount of hemoglobin being attacked is much larger than that of the synthetic hemoglobin, the patient will suffer a certain degree of anemia. Different degrees of systemic coagulation occurred as anemia(32-35), vascular damage, and the body's immune response. Vascular injury may be the principal factor for coagulation in COVID-19 patients who then are under a higher D-Dimer content(36, 37). Studies have showed that the COVID-19 virus also infects T-cells(38), which may cause the abnormal function of T-cells(39). Severe COVID-19 patients often present with mononucleosis(40, 41). Macrophages can engulf free iron, damaged red blood cells and hemoglobin. Of course, macrophages also handle viral inclusions(42), thrombin, fibrin, and foreign matter generated by inflammatory tissues. Thrombin and fibrin may be produced by the coagulation reaction.

If the virus could attack hemoglobin in red blood cells, some prerequisites are necessary here, such as virus infection of red blood cells or hemolysis of red blood cells. There are now some confusing signs. For example, EMMONS, et al. observed that the Colorado tick fever virus existedin red blood cells through electron microscopy(43), which indicates that red blood cells have a risk of infecting some viruses. Mitra, Anupam, et al. found that virus Leukoerythroblastic reaction appeared in a single patient with COVID-19 infection(44). Bhardwaj, et al.pointed out that pRb and its interaction with Nsp15 affect coronavirus infection(45).Recently, it has been reported that the COVID-19 virus infects cells through the Spike-CD147 pathway. CD147 plays an essential role in some systems such as the Ok blood group(46), and T lymphocytes(38). Statistical analysis shows that the susceptibility of COVID-19 has a certain relationship with blood types. The infection rate of blood type A is high, while that of blood type O is minimal. The blood type is an important antigen on the erythrocyte membrane. The latest report shows that the

number of red blood cells in rhesus monkeys infected with the COVID-19 virus is decreasing. However, the mechanism of red blood cell infection by the novel coronavirus remains unclear.

Plasmodium, babesia, and trypanosomes can also infect red blood cells, causing similar symptoms in patients. Trypanosoma extracellular vesicles can also fuse with mammalian red blood cells(47), resulting in the red blood cells to be readily cleared and further leading to anemia. Thrombin sensitization-related adhesion protein and apical membrane antigens are important for babesia invasion of red blood cells(48). There are numerous types of plasmodium, which can infect red blood cells. Plasmodium usually infects red blood cells in three steps. Firstly, it sticks to red blood cells through proteins such as AMA(49). Then, the plasmodium ligand and erythrocyte receptor complete a tight connection. For example, the principal receptor for P. falciparum to invade red blood cells is CD147 protein(50). Finally, dynein, MTRAP (homologous to thrombin-sensitive protein), and other kinetic system proteins finish the process of rapid slide of plasmodium into red blood cells. If the COVID-19 virus also uses thrombin-sensitized protein-mediated sliding into red blood cells, it canaccount for this phenomenon of systemic coagulation in severe patients to a certain extent.

The symptoms of malaria are very similar to those of COVID-19, and there are both symptomatic and asymptomatic infections(51). The SARS-CoV-2 proteins and the Plasmodium falciparum antigen share immunodominant epitopes(52). A computational study found that S, ORF3proteins had Plasmodium antigens rich in tryptophan and threonine. The S protein Plasmodium antigen was the C1q domain, which could bind to the complement receptor 1 on the red blood cell membrane. The Plasmodium antigen of ORF3a were the EBA-175domain, which could bind to glycophorin A on the red blood cell membrane. Then, S protein, ORF3a were attached to band 4.1 to anchor on the erythrocyte membrane skeleton. The invasion would not cause significant hemolysis and hypoxia reactions. According to the SARS-COV-2 Plasmodium antigen type, the blood cells of people with blood type A and Knops were vulnerable to the attack of SARS-COV-2 virus proteins. ORF3a, ORF8, S, and N and others also had more autotransporter domains. So ORF3a and ORF8 proteins could enter the blood and invade red blood cells. ORF3a and ORF8 have domains that bind hemoglobin, then the binding function of heme on hemoglobin may be affected

Heme metabolism is critical for Plasmodium (the causative agent of malaria) infection of erythrocytes(53). Numerous genes encoding potential heme-binding proteins have been identified in the malaria parasite genome(54). Plasmodium requires heme as a metabolic cofactor, and the mitochondria and electron transport chain contain a heme-dependent cytochrome component(55). Plasmodium parasites in the blood stage may not require the electron transport chain to complete the ubiquinone oxidation cycle but rely on heme to manufacture ATP via mitochondrial oxidative phosphorylation(55).The parasite has taken up residence in the red blood cell. Heme is isolated from the host hemoglobin and kept as heme crystals to prevent poisoning by free heme(56). Heme is initially oxidized to yield hematin, which then dimerizes through the reciprocal coordination of iron and propionate moieties(57). Heme is a very hazardous byproduct of hemoglobin metabolism(58). The chelation of heme into heme crystals is the cornerstone of heme detoxification(58). The digestive vacuole stores amorphous heme in hemoglobin, which is then detoxified by the heme detoxification protein. With the assistance of detoxification protein, it is transformed into crystal heme(58). This molecular unit then assembles into Hz crystals that typically take the form of triclinic high aspect ratio parallelograms(57). Chloroquine, a conjugated

antimalarial medication, inhibits heme crystallization, increasing unstable heme(59). There is a method for removing host heme to suit metabolic requirements—mechanism of parasitism(60). Parasites can produce heme from scratch and codes all enzymes involved in the synthesis route (56). Parasites incorporated both host hemoglobin-heme and parasite-synthesized heme into hemozoin and mitochondrial cytochromes(56). Although the heme biosynthesis pathway is not required for the growth of the Plasmodium falciparum parasite's asexual blood stage, it is required for mosquito transmission. Due to the comparable fates of the two heme sources, they may be exploited as a backup method to supply heme during the intra-erythrocyte stage(56).

Heme is a metalloporphyrin compound. Heme induces iron and reactive oxygen species (ROS) Irrelevant signal transduction pathway, which encompasses genes involved in redox metabolism(61). Heme may operate as a danger signal molecule by controlling the quantity of these RNAs(61). Modified porphyrin compounds have been shown to block HIV type 1 gp120 binding to CD4. It thoroughly limits the Env protein's capacity to induce cell fusion with target cells expressing receptors generated via recombinant vectors(62). Heme alone has shown a solid ability to prevent HIV replication. Its concentration was substantially less than that required to inhibit Rauscher murine leukemia virus(63). Additionally, heme induces significant changes in energy metabolism and gene expression associated with immune response, altering susceptibility of bacteria and dengue virus(61). Following hRSV infection, the production of HO-1 with metalloporphyrin cobalt protoporphyrin IX considerably reduced weight loss caused by hRSV-related illnesses. Moreover, HO-1 induction also decreased virus replication and lung inflammation(64) . Antiviral action may be exhibited by heme oxygenase-1 (HO-1). It has been demonstrated that overexpression of HO-1 prevents infection with hepatitis C and B viruses (HCV and HBV), Ebola virus (EBOV), human immunodeficiency virus (HIV), and dengue fever virus (DENV) (65). Zika virus inhibits Heme Oxygenase-1's antiviral action. Once viral replication is established, the level of HO-1 expression is drastically lowered, limiting HO-1's antiviral action(66).

Porphyrin abnormalities are detected in acquired immunodeficiency syndrome(67). And the type of porphyrin metabolic disease induced by the hepatitis C virus is chronic hepatic porphyria, not delayed cutaneous porphyria(67). Patients infected with plasmodium and babesia are treated with chloroquine and quinine, and those infected with trypanosomiasis can be healed with anisace (quinoline pyrimidyl sulfate). Chloroquine is a drug with serious side effects, and part of the earlynovel coronavirus pneumonia has been cured by chloroquine. Perhaps as a result of virus mutation and drug resistance, Chloroquine's therapeutic impact has waned, and there are major adverse effects such as heart damage. Meanwhile, one detail we can notice is that chloroquine is also a commonly used drug for treating porphyria(68, 69). The main symptoms of porphyria appear in the skin and neurovisceral organs. Existing reports show pigmentation in critically ill patients, which however may be a side effect of drugs such as polymyxin B. Some patients with severe skin diseases may also have fever symptoms, which are easily confused with the symptoms of COVID-19 patients(70). Researchers have diagnosed COVID-19 infection with erythema rash, extensive urticaria and chickenpox-like vesicles(71). Some patients with the novel coronavirus pneumonia have similar neurovisceral symptoms. Of course, in the later stage of severe inflammatory infection, the cytokine storm may also induce the failure of many organs. There are symptoms such as diarrhea(72, 73), hypotension(74), and electrolyte disturbances(75). Organs such as hearts(76), livers(77), and kidneys(78) are damaged and develop complications. In terms

of neurological symptoms, some early stealth infections experienced the loss of taste and smell(79, 80). Patients with the severe novel coronavirus pneumonia also suffer from rare neurological diseases such as epilepsy(81, 82) and encephalitis(83, 84). Congenital erythropoietic porphyria due to a genetic defect of the heme biosynthesis enzyme uroporphyrinogen III synthase (85). So the viral proteins had domains that bound porphyrin like uroporphyrinogen III synthase.

The SARS-CoV-2 virus protein combined porphyrin to produce excellent survivability, transmission, and attack power. Most porphyrin molecules are hydrophobic and aggregate in aqueous media(86). The more hydrophobic porphyrin photosensitizer can penetrate the cell membrane of mammalians(87). Due to the concentration gradient, porphyrin also diffuses through the phospholipid bilayer membrane and accumulates in the cytoplasm(88). Porphyrin compounds such as synthetic photosensitizers are commonly adopted in photodynamic therapy for tumors(89). Porphyrin derivatives accumulate in cancer cells through endocytosis and concentration gradient penetration(90). The reactive oxygen species (ROS) produced by porphyrin can kill tumor cells(91). Photodynamic therapy achieves controlled ROS delivery within the cell. The SARS-CoV-2 virus protein-bound porphyrin obtained energy and cell membrane penetration, and generated ROS to damage the cell membrane. SARS-CoV-2 proteins may conduct a series of activities by binding porphyrins. The porphyrin in the human body mainly is stored on hemoglobin in the form of the heme. As the virus requires too many porphyrins, it has evolved the function of attacking the heme on hemoglobin and dissociating iron to form porphyrins. Therefore, we believed that combining viral proteins and porphyrins interfered with the normal heme anabolic pathway of the human body, causing a series of human pathological reactions.

In short, COVID-19 viral protein may conduct a series of activities by binding porphyrins. The porphyrin in the human body mainly is stored on hemoglobin in the form of the heme. As the virus requires too many porphyrins, it has evolved the function of attacking the heme on hemoglobin and dissociating iron to form porphyrins. Because of the severe epidemic, and the existing conditions with limited experimental testing methods for the proteins' functions, it is of great scientific significance to analyze the proteins' function of the novel coronavirus with bioinformatics methods. In this study, conserved domain prediction, homology modeling, and molecular docking techniques were used to analyze the functions of virus-related proteins. The conserved domain analysis showed viral proteins had the ability to attach to porphyrin and produce heme. envelope protein (E) and ORF3a had heme linked sites. ORF3a also possessed the conserved domains of human cytochrome C reductases and bacterial EFeB protein, so that ORF3a could dissociate the heme to iron and porphyrin. This present study revealed that viral proteins could directly bind hemoglobin and S protein could bind extracellular hemoglobin. Besides, ORF3a attacked the 1-beta chain of hemoglobin to dissociate the heme to iron and porphyrin. This mechanism of the virus inhibited the normal metabolic pathway of the heme and made people show symptoms of the disease. Additionally,

2. Methods

2.1 Data set

1. The sequences of SARS-COV-2 proteins. The SARS-COV-2 protein sequences came from the NCBI database. Including: S, E, N, M, ORF3a, ORF8, ORF7a, ORF7b, ORF6, ORF10, orf1ab, orf1a. Among them, the orf1ab and orf1a sequences also included corresponding

subsequences. Since the sequences corresponding to ORF3a's and ORF8's structures in PDB database are missing some fragments, homology modeling of these proteins is required.

2. Related sequences

The related sequence was downloaded from UniProt data set (Table 1).

Table 1. Related sequences are used to search for conserved domains

No	Related protein	Keywords	Count
1	Hemoglobin	Hemoglobin	56,870
2	Porphyrin	Bacterial + porphyrin	30,787
3	cytochrome c	Bacterial+ cytochrome + c	111,967

The protein sequences were also downloaded from NCBI: cytochrome C oxidase, cytochrome D oxidase, Dechelatase proteins. The all sequences were utilized to analyze conserved domains,

3. Crystal structures. At the same time, the PDB files were downloaded from the PDB database: Human Oxy-Hemoglobin 6bb5; DEOXY HUMAN HEMOGLOBIN 1a3n. Some metal porphyrin proteinssuch as human cytochrome, human erythrocyte catalase, Hemocyanin. These proteins are for protein docking with ORF3a or ORF8, respectively.

2.2 A localized MEME tool to identify conserved domains.

The following are the steps involved in the analysis:

1. Downloaded MEME from the official website and installed it in a virtual machine running Ubuntu. VM 15 was the virtual machine.

2. Downloaded the SARS-COV-2 protein sequence from the National Center for Biotechnology Information's official website.

3. Obtained the fasta format sequences of the related protein from the official Uniprot website.

4. Generated fasta format files by MEME analysis for each sequence in all related proteins and each SARS-COV-2 protein sequence.

5. To create multiple batches of the files generated in Step 4, a batch size of 50000 was used. It was limitedby the virtual ubuntu system's limited storage space.

6. Using MEME tools in batches, searched for conserved domains (E-value<=0.05) in SARS-COV-2 and related proteins in Ubuntu.

7. Collected the conserved domains' result files. Located the domain name associated with the motif in the UniProt database.

8. Analyzed the activity of each SARS-COV-2 protein's domains.

2.3 Analysis of conserved domains by online MEME tool

The MEME Suite is an online website that integrates many tools of prediction and annotation motifs. The maximum expectation (EM) algorithm is the basis for MEM's identification of the motif that is a conserved domain of a small sequence in a protein. Motif-based models could assess the reliability of phylogenetic analysis. After opening the online tool MEME, the protein sequences of interest are merged into a text file, and the file format remains fasta. Then, select the number of motifs you want to find, and click the "Go" button. At the end of the analysis, the conserved domains are displayed after clicking the link. The online MEME was used to find the conserved domains of viral proteins by comparing to some metal porphyrin proteins of the bacteria. It is represented that some viral proteins had the heme-linked sites.

2.4 Homology modeling

The quality of ROBETTA modeling is excellent; there are many reference templates, and it can also model some viral proteins with low similarity. After the user submits the sequence online, the server gives a modeling queue. After successful modeling, the server will send the 3D structure file to the submitter's mailbox. This online server also has restrictions on the sequence length. In this study, we modeled the ORF3a, ORF8 sequence with ROBETTA.

2.5 Protein docking technology

The main purpose of protein docking technology is to study the attack of viral proteins onmetal porphyrin proteins such as hemoglobin. Discovery-Studio's ZDOCK is another molecular docking tool for studying protein interactions. Here, it was used to study the attack of hemoglobin by viral non-structural proteins. The following is the docking of ORF3a and hemoglobin, and other docking methods with virus non-structural proteins are the same. After opening the PBD files of Human Oxy-Hemoglobin 6bb5 and ORF3a protein, click the "Dock proteins (ZDOCK)" button of "Dock and Analyze Protein Complexes" under the "macromolecules" menu. In the pop-up interface, select Human Oxy-Hemoglobin 6bb5 as the receptor, and ORF3a as the ligand, and then click the "Run" button. After the computer finishes computing, click on the "protein pose" interface and select the pose and cluster with the highest ZDOCK score. It could obtain the position of ORF3a on Human Oxy-Hemoglobin 6bb5, and Deloxy HUMAN HEMOGLOBIN 1a3n has a similar docking pattern with ORF3a protein.

3. RESULTS

3.1 Viral proteins possess the ability to bind to porphyrin and generate heme.

Porphyrin biosynthesis is the process in mitochondria and cytoplasm. The initial stages of production is in Mitochondria. Three enzymes are involved in the production process: aminolevulinic acid synthase, ALAS1, and ALAS2. In the cytoplasm, the intermediate synthesis stage occurs. Porphobilinogen synthase, porphyrinogen deaminase, uroporphyrinogen III synthetase, and uroporphyrinogen III decarboxylase work sequentially in the synthesis process. The final stage of synthesis occurs in the mitochondria. The production process is carried out sequentially by coproporphyrinogen III oxidase, protoporphyrinogen oxidase, and ferrochelatase. The final product of ferrochelatase is heme The majority of mitochondrial synthesis sites are transmembrane areas. If viral proteins are capable of synthesizing porphyrins, these enzymes should be systematically possessed. The viral membrane is analogous to the mitochondrial transmembrane area, while the viral cytoplasm is analogous. As a result, viruses may be able to generate porphyrins via structural proteins. Because non-structural proteins contain both transmembrane and non-transmembrane proteins, they may also produce porphyrin.

We obtained porphyrin-related sequences from the UniProt database and then compared the viral proteins to the porphyrin-related sequences using the local MEME tool. We combined the motif sequences by protein and domain due to the vast number of motif pieces. Table 2 and Table 3 summarizes the search results. Table 2 shows structural proteins possess enzymes synthesized heme. Table 3 shows non-structural proteins possess enzymes synthesized heme. CysG_dimeriser domain has ferrochelatase activity. Elp3 has the function of coproporphyrinogen III oxidase. GlutR_dimer and GlutR_N are involved in the biosynthesis of tetrapyrrole and have

glutamyl-tRNA reductase and dimerization domain activities. HEM4 has uroporphyrinogen III synthase activity. HemY_N is a bacterial HemY porphyrin biosynthetic protein, which can oxidize coproporphyrinogen III and protoporphyrinogen IX. Porphobil_deam and Porphobil_deamC are porphobilinogen deaminase. TP_methylase is a tetrapyrrole methylase. Uroporphyrinogen_deCOase has uroporphyrinogen decarboxylase activity.

Table 2. SARS-COV-2 structural proteins possess enzymes synthesized heme

Protein	Domain	Motif	Start	End
S	CysG_dimeriser	KRVDFCGKGYH	1038	1048
		ELGKYEQYIKWPWYIW	1202	1217
	Elp3	WFHAIH	64	69
		YYHKNNKSWMESEFRVYSSANNCTFEYVSQPFLMDL EGKQGNF	144	186
		KMSECVLGQSKRVDFCGKGYHLMSFPQSAPH	1028	1058
		QELGKYEQYIKWPWYIWLGFIAGLIAIVMVTIMLCCM TSCCSCLKGCCSCGSCCKFDEDDSEPVLKGVK	1201	1269
	GlutR_N	WFHAIH	64	69
		HWFVTQRNFYEPQ	1101	1113
		KYEQYIKWPWYIW	1205	1217
	HEM4	HKNNKSWM	146	153
		KYEQYIKWPWYIWLGFIAGLIAIVMVTIMLCCMTSCCS CLKGCCSCGSCCKFDE	1205	1258
	HemY_N	GKYEQYIKWPWYIWLGFIAGLIAIVMVTIMLCCMTSC CSCLKGCCSCGSCCK	1204	1255
	Porphobil_deam	VYYHKNNKSWM	143	153
		KYEQYIKWPWYIWLGFIAGLIAIVMVTIMLCCM	1205	1237
	Porphobil_deam C	YYHKNNKSWM	144	153
		KYEQYIKWPWYIWLGFIAGLIAIVMVTIMLCCMTSCCS CLKGCCSCGSCC	1205	1254
	TP_methylase	MQMAYR	900	905
		GKYEQYIKWPWYIWLGFIAGLIAIVMVTIMLCCMTSC CSCLKGCC	1204	1248
	Uroporphyrinog en_deCOase	TWFHAIHV	63	70
		YYHKNNKSWMESEFR	144	158
		WNRKRIS	353	359
		PFAMQMAYR	897	905
		CGKGYHLM	1043	1050
		PAICHDGKAHFPREGVFVSNGTHWFVTQRNFYEP	1079	1112
		IDLQELGKYEQYIKWPWYIWLGFIAGLIAIVMVTIMLC CMTSCCSCLKGCCSCGSCCKFDEDD	1198	1260
E	CysG_dimeriser	LCAYCCNIVN	39	48
	Elp3	TLAILTALRLCAYCCNIVNVSLVKPSFYVYSRVKNLNS S	30	68
	GlutR_dimer	CAYCCNIVNVSLVKPSFY	40	57
	GlutR_N	TALRLCAYCCNIVNVSLVKPSFYVYSRVKNLNS	35	67

	HEM4	RLCAYCCNIVNVSLVKPSFYVYSRVKN	38	64
	HemY_N	CAYCCNIVNVSLVKPSFYVYSRVK	40	63
	Porphobil_deam	ILTALRLCAYCCNIVNVSLVKPSFYVYSRVKNLNSS	33	68
	Porphobil_deam C	TALRLCAYCCNIVNVSLVKPSFYVYSRVKNLNSS	35	68
	TP_methylase	RLCAYCCNIVNVSLVKPSFYVYSRVKNLNSSRVPD	38	72
	Uroporphyrinogen_deCOase	TLAILTALRLCAYCCNIVNVSLVKPSFYVYSRVKNLNSSR	30	69
M	Elp3	SMWSFNPETNILLNVPLH	108	125
		HLRIAGHHLGRCDIKDLPKEITVATS	148	173
		YSRYRIGNYKLNTDHSSSSDN	196	216
	GlutR_N	MACLVGLMW	84	92
		MWSFNPE	109	115
	HEM4	MWSFNPET	109	116
	Porphobil_deam	MWSFNPE	109	115
		HHLGRCDIKDLPKE	154	167
	TP_methylase	CDIKDLPKEITVATSRTLSYYK	159	180
		KLNTDHSSSSDNI	205	217
	Uroporphyrinogen_deCOase	SMWSFNPE	108	115
		HHLGRCD	154	160
N	Elp3	NNTASWFTALTQH	47	59
		DLKFPRGQGVPINTNSSPDDQIGYYRRATRRIRGGDGK	63	146
		MKDLSPRWYFYYLGTGPEAGLPYGANKDGIIWVATE		
		GALNTPKDHI		
		IRQGTDYKHWPQIAQFAPSASAFFGMSRIGMEVTPSGT	292	379
		WLTYTGAIKLDDKDPNFKDQVILLNKHIDAYKTFPPTE		
		PKKDKKKKADET		
	GlutR_N	MKDLSPRWYFYYLGTGPE	101	118
		IRQGTDYKHWPQI	292	304
		SGTWLTYTGAIKLDDKDPNFKDQVILLNKHIDAY	327	360
	HEM4	MKDLSPRWYFYYLG	101	114
		DYKHWPQI	297	304
		FKDQVILLNKHIDAYKTF	346	363
	Porphobil_deam	RWYFYYL	107	113
		DYKHWPQIAQFAPSASAFFGMSRIGMEV	297	324
		KHIDAYKTFPP	355	365
	TP_methylase	MKDLSPRWYFYYL	101	113
		IRQGTDYKHWPQIAQFAPSASAFFGMSRIGMEV	292	324
	Uroporphyrinogen_deCOase	GDGKMKDLSPRWYFYYL	97	113
		PRQKRTATKAYNVTQAFGRRGPEQTQGNFGDQELIRQ	258	305
		GTDYKHWPQIA		
		MSRIGMEVTPSGTWLTYT	317	334

Table 3. SARS-COV-2 non-structural proteins possess enzymes synthesized heme

Protein	Domain	Motif	Start	End
ORF3a	CysG_dimeriser	CWKCRSKNPLLYDANYFLCWHTNCYDYCIPY	130	160
	Elp3	QSINFVRIIMRLWLCWKCRSKNPLLYDANYFLCWHTN CYDYCIPYNSV	116	163
	GlutR_N	IMRLWLCWKCRSKNPLLYDANYFLCWHTNCYDYCIP YNSV	124	163
	HEM4	NFVRIIMRLWLCWKCRSKNPLLYDANYFLCWHTNCY DYCIPYN	119	161
	HemY_N	WKCRSKN	131	137
		NYFLCWHTNCYDYCIPYN	144	161
	Porphobil_deam	MRLWLCWKCRSKNPLLYDANYFLCWHTNCYDYCIPY NS	125	162
	Porphobil_deamC	MRLWLCWKCRSKNPLLYDANYFLCWHTNCYDYCIPY N	125	161
	TP_methylase	NFVRIIMRLWLCWKCRSKNPLLYDANYFLCWHTNCY DYCIPYN	119	161
	Uroporphyrinogen _deCOase	YFLQSINFVRIIMRLWLCWKCRSKNPLLYDANYFLCW HTNCYDYCIPYNS	113	162
ORF6	CysG_dimeriser	WNLDYIIN	27	34
	Elp3	MFHLVDFQVTIAEILLIIMRTFKVSIWNLDYIINLIIKNLS KSLTENKYSQLDEEQPMEID	1	61
	GlutR_N	MFHLVDFQVTIAEILLIIMRTFKVSIWNLDYIINLIIKNLS KSLTENKYSQLDEEQPMEID	1	61
	HEM4	MFHLVDFQVTIAEILLIIMRTFKVSIWNLDYIINLIIKNLS KSLTENKYSQLDEEQPM	1	58
	HemY_N	FQVTIAEILLIIMRTFKVSIWNLDYIINLIIKNLSKSLTEN KYS	7	50
	Porphobil_deam	MFHLVDFQVTIAEILLIIMRTFKVSIWNLDYIINLIIKNLS KSLTENKYSQLDEEQPME	1	59
	Porphobil_deamC	TFKVSIWNLDYIINLIIKNLSKSLTENKYSQLDEEQPME	21	59
	TP_methylase	MFHLVDFQVTIAEILLIIMRTFKVSIWNLDYIINLIIKNLS KSLTENKYSQLDEEQPMEID	1	61
	Uroporphyrinogen _deCOase	MRTFKVSIWNLDYIINLIIKNLSKSLTENKYSQLDEEQP ME	19	59
ORF7a	Elp3	TCELYHYQECVRGT	14	27
		TYEGNSPFHPLADNKFALTCFSTQFAFACPDGVKHVY Q	39	76
	GlutR_N	TCELYHYQECVRGTTVLLKEPCSSGTYEGNSPFHPLAD NKFALTCFSTQFAFACPDGVKHVYQLRARSVSPKLF	14	87
	HEM4	TCELYHYQEC	14	23
		KEPCSSGTYEGNSPFHPLADNKF	32	54
		QFAFACPDGVKHVYQ	62	76
	HemY_N	PCSSGTYEGNSPFHPLADNKFALTCFSTQFAFAC	34	67

	Porphobil_deam	CELYHYQECVRGTTVLLKEPCS	15	36
	Porphobil_deamC	YHYQEC	18	23
		NSPFHPLADNKFALTC	43	58
	TP_methylase	YHYQEC	18	23
		YEGNSPFHPLADNKFALTCFSTQ	40	62
		SVSPKLFIRQEEVQELYSPI	81	100
	Uroporphyrinogen_deCOase	ATCELYHYQECVRGTTVLLKEPCSSGTYEGNSPFHPLADNKFALTCFSTQFAFACPDGVKHVYQLR	13	78
ORF7b	CysG_dimeriser	DFYLCFLAFLLFLVLIMLIIFWFSLELQDHNETCH	8	42
	Elp3	MIELSLIDFYLCFLAFLLFLVLIMLIIFWFSLELQDHNETCH	1	42
	GlutR_N	MIELSLIDFYLCFLAFLLFLVLIMLIIFWFSLELQDHNETCH	1	42
	HEM4	MIELSLIDFYLCFLAFLLFLVLIMLIIFWFSLELQDHNETCHA	1	43
	HemY_N	IDFYLCFLAFLLFLVLIMLIIFWFSLELQDHNETCH	7	42
	Porphobil_deam	MIELSLIDFYLCFLAFLLFLVLIMLIIFWFSLELQDHNETCHA	1	43
	Porphobil_deamC	IMLIIFWFSLELQDHNETCHA	23	43
	TP_methylase	MIELSLIDFYLCFLAFLLFLVLIMLIIFWFSLELQDHNETCHA	1	43
	Uroporphyrinogen_deCOase	MIELSLIDFYLCFLAFLLF	1	19
		IMLIIFWFSLELQDHNETCHA	23	43
ORF8	CysG_dimeriser	HFYSKWYI	40	47
	Elp3	MKFLVFLGIITTVAAFHQECSLQSCTQHQPYVVDDPCPIHFYSKWYIRVGARK	1	53
		CVDEAGSKSPIQYIDIGNYTVSCLPFTINCQEPKLGSLVVRCSFY	61	105
	GlutR_N	CSLQSCTQHQPYVVDDPCPIHFYSKWYIRVGA	20	51
		KSPIQYIDIGNYTVSCLPFTINCQEPK	68	94
	HEM4	QSCTQHQPYVVDDPCPIHFYSKWYIRVGARK	23	53
	HemY_N	PIHFYSKWYIR	38	48
		SKSPIQYIDIGNYTVSCLPFTINCQEPK	67	94
	Porphobil_deam	SCTQHQPYVVDDPCPIHFYSKWYIR	24	48
		IELCVDEAGSKSPIQYIDIGNYTVSCLPFTINCQEPK	58	94
	Porphobil_deamC	TVAAFHQECSLQSCTQHQPYVVDDPCPIHFYSKWY	12	46
	TP_methylase	FHQECSLQSCTQHQPYVVDDPCPIHFYSKWYIRVGARK	16	53
		KSPIQYIDIGNYTVSCLPFTINCQEPKLGSLVVRCSFYEDFLEY	68	111
	Uroporphyrinogen_deCOase	FHQECSLQSCTQHQPYVVDDPCPIHFYSKWYIRVGAR	16	52
		GSKSPIQYIDIGNYTVSCLPFTINCQ	66	91

ORF10	CysG_dimeriser	FAFPFTIYSLLLCRMNSRNYI	7	27
	Elp3	MGYINVFAFPFTIYSLLLCRMNSRNYIAQVDVVNFN	1	36
	GlutR_N	MGYINVFAFPFTIYSLLLCRMNSRNYIAQVDVVNFN	1	36
	HEM4	MGYINVFAFPFTIYSLLLCRMNSRNYIAQVDVVNFNL	1	37
	HemY_N	MGYINVFAFPFTIYSLLLCRMNSRNYIAQVDVVNF	1	35
	Porphobil_deam	MGYINVFAFPFTIYSLLLCRMNSRNYIAQVDVVNFN	1	36
	Porphobil_deamC	MGYINVFAFPFTIYSLLLCRMNSRNYIAQVDVVNFNLT	1	38
	TP_methylase	MGYINVFAFPFTIYSLLLCRMNSRNYIAQVDVVNFNL	1	37
	Uroporphyrinogen_deCOase	MGYINVFAFPFTIYSLLLCRMNSRNYIAQVDVVNFN	1	36
nsp2	Elp3	RGVYCCREHEHEIAWY	46	61
		CHNKCAYW	236	243
	GlutR_N	CCREHEHEIAW	50	60
	Porphobil_deam	CCREHEHE	50	57
	TP_methylase	REHEHEIAW	52	60
	Uroporphyrinogen_deCOase	YCCREHEHEIAWYTERS	49	65
nsp3	HEM4	NTWCIRCLW	1188	1196
	HEM4	WLMWLIINLVQMAPISAMVRMYIFFASFYYVW	1545	1576
	TP_methylase	ACIDCSARHINAQVAKSHNIALIW	1872	1895
	Uroporphyrinogen_deCOase	GRYMSALNHTKKWKYPQVNGLTSIKWADNNCY	826	857
nsp4	Elp3	AHIQWMVMFTPLVPFWITIAYIICISTKHFYWFFS	361	395
	HEM4	AHIQWMVMFTPLVPFWITI	361	379
nsp6	CysG_dimeriser	WVMRIMTW	90	97
	Uroporphyrinogen_deCOase	AYFNMVYMPASWVMRIMTWLDM	79	100
nsp10	Elp3	SCCLYCRCHIDHPN	72	85
	HEM4	YCRCHIDHPNP	76	86
2'-O-ribose methyltransferase	Elp3	AMPNLYKMQRM	10	20
	Uroporphyrinogen_deCOase	MGHFAWW	184	190
3C-like proteinase	GlutR_N	YMHHME	161	166
3'-to-5' exonuclease	CysG_dimeriser	AKPPPGDQFKHLIPLMYKGLPW	138	159
	Elp3	CWHHSIGFDYVYNPFMIDVQQWGFTGNLQSNHDLYCQVHGNAH	226	268
	GlutR_N	YACWHH	224	229

	HEM4	GYPNMFITREEAIRHVRAW	68	86
		WHHSIGFDYVYNPFMIDVQQWGFTGNLQSNH	227	257
		HHANEYRLYLDAYNMMISAGFSLWVYKQF	486	514
	TP_methylase	PPPGDQFKHLIPLMYKGLPWNVVR	140	163
	Uroporphyrinogen _deCOase	MGFKMNYQVNGYPNMFITREEAIRHVRAWIGFDVEG CH	58	95
		WHHSIG	227	232
		CRHHANEY	484	491
helicase	Elp3	RCGACIRRPFLCCKCCYDHVISTSHK	15	40
	Uroporphyrinogen _deCOase	GPDMFLGTCRRC	433	444
leader protein	Uroporphyrinogen _deCOase	PHGHVM	80	85
RdRP	Elp3	PHEFCSQHTMLVKQGDDYVYLPYP	809	832
	Porphobil_deam	ENPHLMGWDYPKCDRAMPNM	610	629
	Uroporphyrinogen _deCOase	YSDVENPHLMGWDYPKCDRAMPNMLRIMA	606	634

Porphyrinogen deaminase, uroporphyrinogen III synthase, uroporphyrinogen III decarboxylase, and coproporphyrinogen III oxidase domains are present in both structural and non-structural proteins, as shown in Table 2 and Table 3. There were ferrochelatase domain present. It indicates that structural and non-structural proteins can employ porphobilinogen as a starting material for synthesizing heme, respectively. Multiple viral proteins collaborate to finish the porphyrin production pathway. Due to the limitations of our analysis capabilities, we cannot determine the relation of porphyrin synthesis between viral proteins. These enzyme activity domains are linked to porphyrin. As a result, viral proteins can also interact with porphyrins via these enzyme domains.

3.2 Viral proteins can bind hemoglobin

Eryth_link_C is on the linker subunit of the giant extracellular hemoglobin (globin) respiratory complex. The linker subunit's C-terminal globular domain is involved in trimerization. It also interacts with globin and other adjacent trimers' C-terminal spherical linker domains. In Staphylococcus aureus, the NEAT domain encodes the human hemoglobin receptor. The NEAT domain recognizes a subfamily of iron-regulated surface determinant proteins that are found exclusively in bacteria. Iron-regulated surface determining protein H (isdH, also known as harA) interacts with the human plasma haptoglobin-hemoglobin complex, haptoglobin, and hemoglobin. It has a much higher affinity for haptoglobin-hemoglobin complexes than haptoglobin alone. These three domains serve distinct purposes. IsdH(N1) binds hemoglobin and haptoglobin; IsdH(N3) binds heme that has been released from hemoglobin.

We downloaded hemoglobin-related sequences from the UniProt database. We then compared the viral proteins to the hemoglobin-related sequences using the local MEME version. We combined the motif sequence by protein and domain due to the vast number of motif pieces. Table 4 summarizes the search results. S, E, N, orf3a, orf6, orf7a, orf7b, orf8, orf10, 2'-O-ribose methyltransferase contain NEAT domains, as shown in Table 4. The domain Eryth_link_C is present in S, N, orf6, orf7b, orf8, orf10, nsp6, nsp10, and RdRP. Both Eryth link C and NEAT domains are in S, N, orf6, orf7b, orf8, orf10, respectively. Because S can form a trimer structure, it

can be combined with extracellular hemoglobin. The S Eryth_link_C A is involved in receptor binding. S Eryth_link_C B is a member of the S2 family of proteins involved in membrane integration. The NEAT domains of S, E, N, orf3a, orf6, orf7a, orf7b, orf8, orf10, and 2'-O-ribose methyltransferase may perform distinct functions. S NEAT A and S Eryth_link_C B are mutually overlapped. E NEAT A is shorter proteins that perform the function of heme capture. S, N, orf3a, orf6, orf7b, orf8, orf10 have a longer NEAT capable of binding and capturing hemoglobin.

Table 4. The SARS-COV-2 virus protein contains the Eryth_link_C and NEAT domains.

Protein	Domain	Alia	Motif	Start	End
S	Eryth_link_C	A	CEFQFCNDPFLGVYYHKNNKSWMESEFR	131	158
		B	YIKWPWYIWL	1209	1218
	NEAT	A	KWPWYIWLGFIAGLIAIVMVTIMLCCMT	1211	1238
E	NEAT	A	LRLCAYCC	37	44
N	Eryth_link_C	A	YKHWPQIAQF	298	307
	NEAT	A	RWYFYY	107	112
		B	ELIRQGTDYKHWPQI	290	304
ORF3a	NEAT	A	NFVRIIMRLWLCWKCRSKNPLLYDANYFLC WHTNCYDYCI	119	158
ORF6	Eryth_link_C	A	ILLIIMRTFKVSIWNLDYIINLIIKNLSKSLTEN KYSQLDEEQPMEI	14	60
	NEAT	A	ILLIIMRTFKVSIWNLDYIINLIIKN	14	39
ORF7a	NEAT	A	CELYHYQECVR	15	25
ORF7b	Eryth_link_C	A	MLIIFWFSLELQDHNETCH	24	42
	NEAT	A	MLIIFWFSLELQDHNETCHA	24	43
ORF8	Eryth_link_C	A	AFHQECSLQSCTQHQPYVVDDPCPIHFYSKW YIRVGARK	15	53
	NEAT	A	FHQECSLQSCTQHQPYVVDDPCPIHFYSKWYI RVGARKSAPLIELCVDEAGSKSPIQYID	16	75
ORF10	Eryth_link_C	A	MGYINVFAFPFTIYSLLLCRMNSRNYIAQVDV VNF	1	35
	NEAT	A	MGYINVFAFPFTIYSLLLCRMNSRNYIAQVDV VNFN	1	36
nsp6	Eryth_link_C	A	FNMVYMPASWVMRIMTW	81	97
nsp10	Eryth_link_C	A	FGGASCCLYCRCHIDH	68	83
RdRP	Eryth_link_C	A	ENPHLMGWDYPKCDRAMPNMLRIM	610	633
2'-O-ribose methyltrans ferase	NEAT	A	MGHFAWWTAF	184	193

3.3 The Haem_bd domain of viral proteins can bind heme.

The UniProt database was used to find cytochrome C-related sequences. Then we adopted the local version of MEME to match the viral proteins and cytochrome C-related sequences. Due to a large number of motif fragments, we organized motif sequences by protein and domain. Table 5 displays the search results. S, N, E, orf3a, orf7b, orf10, nsp2, nsp3, and RdRP all have Haem_bd domains, as seen in Table 5. A possible heme-binding motif CXXCH can be found in the

Haem_bd (PF14376) domain. H connects to the iron in heme, while two Cs bind to porphyrin(92). The Haem_bd domain is found in most cytochrome C oxidases. It demonstrates that the Haem bd domain of these viral proteins can bind heme.

Table 5. Haem_bd domain of SARS-COV-2 viral protein

Protein	Alias	Haem_bd Motif	Start	END
S	A	WFHAIH	64	69
	B	NFTTAPAICHDGKAHFPRE	1074	1092
	C	GKYEQYIKWPWYIWLGFIAGLIAIVMVTIMLCCM	1204	1237
E	A	RLCAYCC	38	44
N	A	PRWYFYYLGTGPEAGLPYGANKDGIIWVATEGALNTPKDH	106	145
	B	QGTDYKHWPQIAQFAPSASAFFGMSRIGMEVTPSGTWLTY	294	333
	C	VILLNKHIDAYKTFPPTE	350	367
orf3a	A	NFVRIIMRLWLCWKCRS	119	135
	B	NCYDYC	152	157
orf7b	A	QDHNETCH	35	42
orf10	A	CRMNSRNY	19	26
nsp2	A	KRGVYCCREHEHEIAWYTERSEKSYELQTPFE	45	76
nsp3	A	CASEYTGNYQCGHYKHI	1005	1021
RdRP	A	PHLMGWDYPKCDRAMPNMLRIMASLVLARKH	612	642

According to the motif CXXCH of the linked sequences, we formed a one-to-one correlation with the results in Table 5, and then sorted out the Haem motif (Table 6). Only E and ORF3a carry the CXXC motif, as shown in Table 6. Hematoporphyrin binds both C molecules. E has C44 as Fe binding sites, and ORF3a has R134. But neither does H. This mutation may make it easier for viral proteins to bind iron. E and ORF3a bind to heme in a relatively steady manner. Other viral proteins' heme-binding could be unstable.

Table 6. The Haem motif of CXXCH is in the SARS-COV-2 viral protein.

Protein	Alias	Haem motif	Start-End	Haem-Fe Site
S	A	PAICH	1079-1083	H1083
	B	KYEQY	1205-1209	Y1209
E	A	CAYCC	40-44	C44
N	A	WYFYY, YYLGT	108-112, 111-115	Y112, T115
	B	TDYKH, DYKHW	296-300, 297-301	H300, W301
	C	NKHID, HIDAY	354-358, 356-360	D358, Y360
ORF3a	A	CWKCR	130-134	R134
	B	CYDYC	153-157	C157
ORF7b	A	NETCH	38-42	H42
nsp2	A	VYCCR	228-232	R232
nsp3	A	CASEY	1823-1827	Y1827

3.4 Heme linked and Electronic transmission motif of ORF3a

We will further study the heme binding sites of orf3a and E protein. It was noticed that there was a phenomenon, in which some bacteria degrade the heme to form porphyrin rings and iron. These bacteria hunt for iron for survival. There are two primary forms of bacteria degrading the heme. To be specific, one is heme oxidase-mediated, while the other is a heme-degrading enzyme.

Both methods have one thing in common, starting with trivalent iron andthe heme, and dissociating iron through complex electron transfer, oxidation, reduction, and cracking processes. In the heme oxidase-mediated manner, the process of electron transfer is achieved through cytochrome reductases. If the viral protein dissociates the iron of the heme, it may have a partially conserved domain of cytochrome oxidoreductase. There are tens of thousands of bacteria, and it is impossible to compare them one by one. In this case, only representative bacteria are selected.

If viral proteins attack hemoglobin and the heme, iron, carbon dioxide, and oxygen are produced. The human body may be a hostile environment lacking oxygen, acidity, iron, and oxygen-free radicals. Viral proteins may have similar capabilities to the proteins of some extreme environmental bacteria. The members of Aquificales are the bacterial communities known to have higher growth temperatures so far, andthey are widely distributed around the world, mainly growing in volcanic or geothermally heated environments. Here, the Hydrogenobaculum was selected as a reference, and it plays an essential role in the biogeochemical cycle of these hot springs. Hydrogenobaculum (strain Y04AAS1) was a thermophilic acidophilic bacterium, and was isolated from the Earth Hot Springs, such as the obsidian pool of Yellowstone National Park. It grows optimally at 58°C and pH4, and gains energy through the oxidation of hydrogen (the "knallgas" reaction) or reduced sulfur compounds.

Exposure to the conserved domain of heme linked sites. We downloaded the sequence cytochrome C oxidases (gi | 452882433 | gb | AGG15137 |, AGG15137.1, cytochrome C oxidase monoheme subunit / FixO [Hydrogenobaculum sp. HO]) and its' related structure 3MK7B from NCBI. Then, in this study, the MEME tool was used to compare cytochrome Coxidases with viral proteins to find conserved domains. After that, it was found that ORF3a and cytochrome C oxidases have the conserved domain "IMRAWGCWKCR" (Figure 1.A), E value = 2.0E-003<0.05, which has a certain statistical significance. The sequence position of the conserved domain in AGG15137.1 is 111-121 (Figure 1.B), which belongs to the front of the cytochrome oxidase domain pfam02433 listed by NCBI.

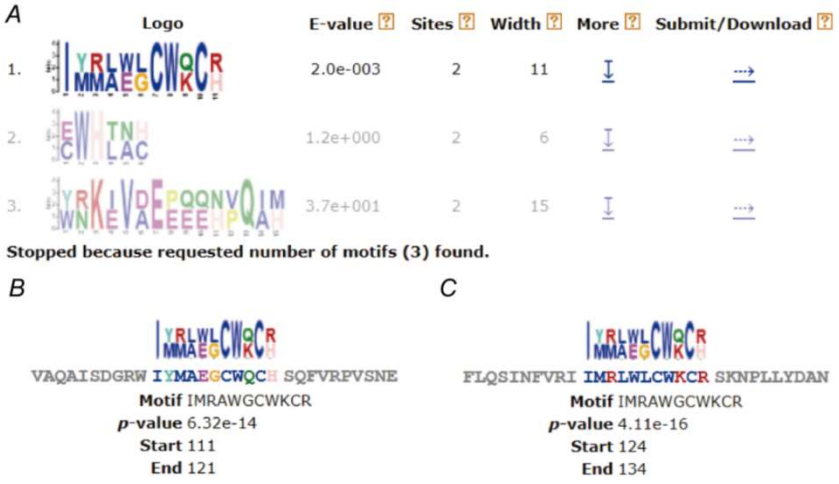

Figure 1. Heme-linkeddomain of ORF3a**.** ***A***. Heme-linkeddomain"IMRAWGCWKCR". *B*. heme linked sites at positions 111-121 of AGG15137.1. *C*. heme linked sites at positions 124-134 of ORF3a.

We displayed 3MK7B in the Cn3D tool and looked at the structure area at positions 111-121 (Figure 2.). The yellow area in Figure 2.A is the functional area of the conserved domain "IMRAWGCWKCR", which connects the heme iron, the carbon at the left end of the alpha position, and the beta position(Figure 2.A).

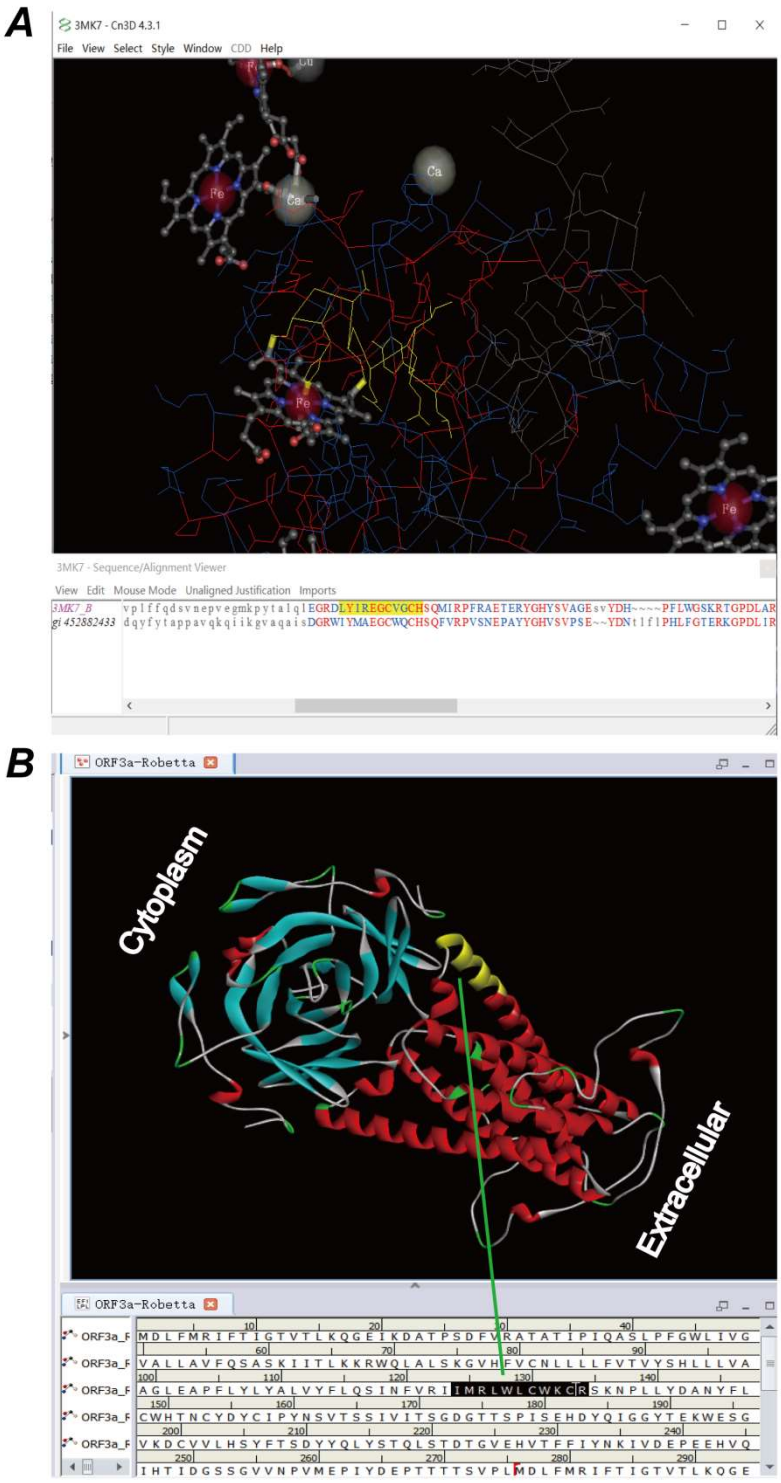

Figure 2. 3D position of heme motif. ***A***. 3D position of heme motif in 3MK7B. ***B***. 3D position of heme motif in ORF3a. The ORF3a is a dimer. This figure depicts a heme motif of one monomer. The other monomer's heme motif is in a similar site. The heme motif(IMRLWLCWKCR) is across the inner membrane and the cytoplasm.

In other words, the last Arg of the conserved domain corresponds to the His of 3MK7B. His nitrogen atom connected to iron(Figure 2.A), and can cooperate with metal ions such as iron. For example, the link of the heme to myoglobin or hemoglobin was formed by histidine and iron asthe coordination key. The last two Cys connected the second carbon at the left end of the alpha position and the beta position. The first Cys connected the second carbon at the end of the alpha position, while the second Cys connected the second carbon at the end of the beta position. The sequence position of the conserved domain "IMRAWGCWKCR" in ORF3a is 124-134 (Figure 1.C), which belongs to the active area of ORF3a (Figure 2.B).

The result indicated that Arg134 of ORF3a linked to the iron of the heme, and Cys130 and Cys133 linked to the carbon at the left end of the alpha position and the beta position respectively(Figure 3). It is interesting that cytochrome C oxidases and ORF3a linked the heme at alpha and beta areas with Cys, indicating that this position may be highly conserved. ORF3a's iron linker evolved from His to Arg.

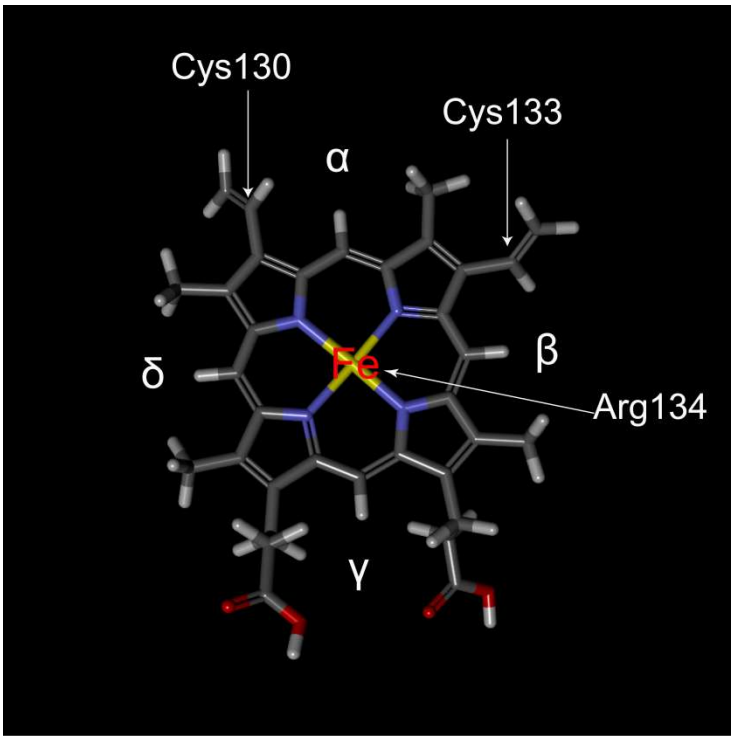

Figure 3. Heme linked positions for ORF3a

The conservative domain of electronic transmission. At present, the detail mechanism of electron transmission in cells is not yet clear. The electron transfer related heme is divided into two parts: from the electron donor to the low-rotation heme and from the low-rotation heme to the binuclear center. The first part can be a multi-step process and varies between different families, while the second part (direct transfer) is consistent throughout the superfamily. It was believed here that ORF3a must have a conserved domain of human cytochrome C oxidases in order to have limited electron transport capabilities. Then, the MEME tool was used to compare ORF3a with human cytochrome C oxidases (AGW78696.1 cytochrome C oxidase subunit I (mitochondrial) [Homo sapiens]). Therefore, it was found that both have a conservative domain "RJWECWKCKRKNPLLEEPNMNLCWHYGCPDPC", E value = 1.0E-002<0.05 (Figure 4.A), which has certain statistical significance. The domain of cytochrome C oxidases is 471-502 (Figure 4.B), which is the active region for electron transport. The ORF3a site is 126-157 (Figure

4.C), including the conserved domain exposed to the heme, while Cys130, Cys133, and Arg134 are still conserved sites in the electron transport domain.

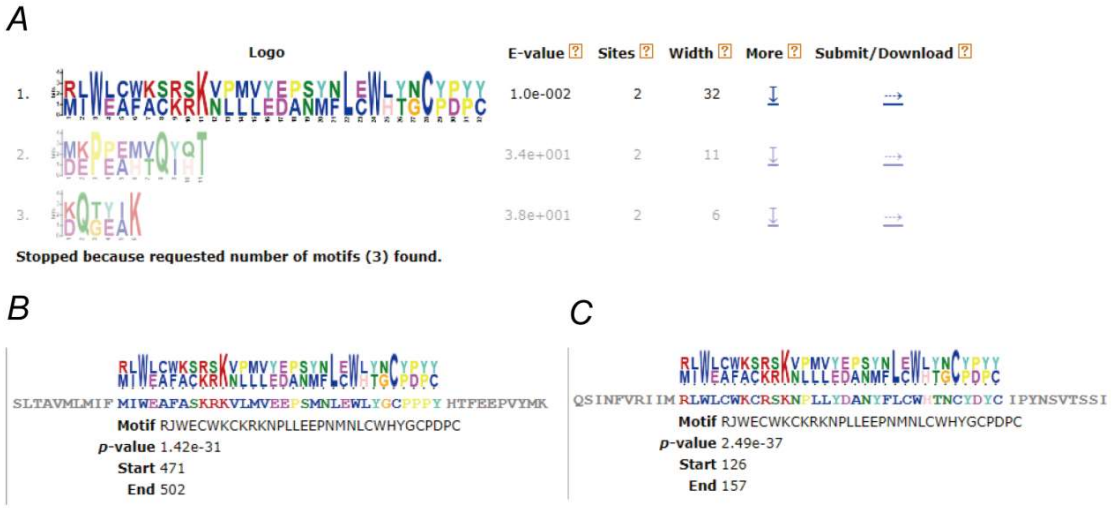

Figure 4. Electronic transmission domain of ORF3a. ***A***. Electronic transmission domain"RJWECWKCKRKNPLLEEPNMNLCWHYGCPDPC". ***B***. Electronic transmission sites at positions 471-502 of AGW78696.1. ***C***. Electronic transmission sites at positions 126-157 of ORF3a.

Bacterial control group analysis. To prove that the above analysis is not accidental, a comparative analysis was conducted. Firstly, MEME was used to compare the domains of cytochrome oxidase of Aquificales and viral proteinsORF3a. Then, two types of bacteria, the positive pair of bacteria (Table 7) such as Hydrogenophilus and the negative control bacteria (Table 8) such as Mycobacterium tuberculosiswere randomly selected. For the two types of bacteria, the domains of cytochrome oxidases were searched separately, and the E-value of many results was greater than 0.05, or no conserved heme domain was found. It indicates that ORF3a protein may dissociate the iron from the heme in an ancient way, which is different from the general bacterial protein. The electron transport region partially overlapped with cytochrome c oxidase subunit I of Legionella and Streptococcus pneumoniae, where the viral pneumonia condition was similar to two bacteria infections.

Table 7. conserved domain between Cytochromeoxidase of Aquificales and ORF3a

ID	Species	Protein	E-value	Positions of oxidase	Positions of ORF3a
AAC07899.1	Aquifex aeolicus VF5	cytochrome c oxidase subunit I	3.00E-03	472-481	148-157
BBD76882.1	Hydrogenophilus thermoluteolus	cytochrome b561	3.20E+00	-	-
AAP84291.1	Terricola subterraneus	cytochrome b, partial	3.00E-01	-	-
Q56408.2	COX1_THETH Thermus_thermophilus	Cytochrome c oxidase subunit 1	8.10E-01	-	-
Q5SJ79.1	COX1_THET8 Thermus_thermophilus_HB8	Cytochrome c oxidase subunit 1	1.40E+00	-	-
AOV85240.1	Zelotes subterraneus	cytochrome oxidase subunit 1, partial	4.90E+00	-	-

Table 8. conserved domain between Cytochromeoxidase of bacteria and ORF3a

ID	Species	Protein	E-value	Positions of oxidase	Positions of ORF3a
NP_705912.1	Cryptococcus neoformans var. grubii	Cytochrome c oxidase subunit 1	4.60E-01	-	-
PCQ20475.1	Klebsiella pneumoniae	Cytochrome c oxidase subunit 1	1.30E+00	-	-
WP_027270427.1	Legionella	Cytochrome c oxidase subunit 1	1.80E-02	420-429	148-157
VCU51329.1	Mycobacterium tuberculosis	Cytochrome c oxidase subunit 1	2.70E-01	-	-
AVZ37898.1	Pseudomonas aeruginosa	Cytochrome-c oxidase	5.90E-01	-	-
WP_025904654.1	Staphylococcus	Cytochrome c oxidase subunit 1	1.00E+00	-	-
COP70899.1	Streptococcus pneumoniae	Cytochrome c oxidase subunit 1	2.20E-02	512-536	113-137
AAK33439.1	Streptococcus pyogenes M1 GAS	hypothetical protein SPy_0407	2.20E+00	-	-

Coronavirus control group analysis. To prove that the heme linked sites of ORF3a evolved from bats, the ORF3/ORF3a proteinsof several coronaviruses, SARS virusesand MERS viruses were analyzed by comparing with FixO (AGG15137.1 cytochrome C oxidase mono-heme subunit/FixO [Hydrogenobaculum sp. HO]) (Table 9). Table 9 shows that ORF3/ORF3a of coronavirus and MERS viruses has no conserved domains of heme linked sites. Table 9 shows that ORF3a of the SARS virus in various animals has a conserved domain of heme linked sites.

ORF3a protein may kick off the iron of the heme through electron transfer, oxidation and reduction. The attack of ORF3a on the heme is consistent with the research report of ORF3a causing apoptosis. the heme can regulate apoptosis through cytochrome C and other molecules. We checked the conserved domain of the ORF3a protein from NCBI, and the results showed that the ORF3a protein belongs to the APA3_viroporin super family (number: pfam11289) that is a pro-apoptotic protein. The severe acute respiratory syndrome coronavirus (SARS-CoV) causes apoptosis of infected cells, which is one of the culprits. Therefore, the iron dissociated from the heme by ORF3a may be the direct cause of apoptosis.

Table 9. Heme linked motifs in ORF3/ORF3a protein of some coronavirus

No.	ID	Species	Protein	E-value	Positions of FixO	Positions of ORF3/ORF3a	Motif
1	AYV99804.1	SARS coronavirus Urbani	ORF3a	1.40E-03	111-121	124-134	IMRCWGCWKCK
2	AAP72975.1	SARS coronavirus HSR 1	ORF3a	1.40E-03	111-121	124-134	IMRCWGCWKCK
3	AAP33698.1	SARS coronavirus Frankfurt 1	ORF3a	1.40E-03	111-121	124-134	IMRCWGCWKCK
4	AAU04650.1	SARS coronavirus civet010	ORF3	7.50E-04	111-121	124-134	IMRCWGCWKCK
5	AAQ94061.1	SARS coronavirus AS	ORF3a	1.40E-03	111-121	124-134	IMRCWGCWKCK
6	AAV91632.1	SARS coronavirus A022	ORF3	5.10E-04	111-121	124-134	IMRCWGCWKCK
7	AAU04635.1	Civet SARS CoV 007/2004	ORF3	5.10E-04	111-121	124-134	IMRCWGCWKCK
8	ATO98232.1	Bat SARS-like coronavirus	ORF3a	1.50E-03	111-121	124-134	IMRCWGCWKCK
9	YP_003858585.1	Bat coronavirus BM48-31/BGR/2008	ORF3	5.10E-04	111-121	124-134	IMRCWGCWKCK
10	QIA48642.1	Pangolin coronavirus	ORF3a	2.80E-03	111-121	124-134	IMRAWGCWKCR
11	APD51508.1	229E-related bat coronavirus	ORF3	2.50E-02	108-121	104-117	GRWFHMAWGCWQCK
12	AZF86131.1	Alphacoronavirus Bat-CoV/P.kuhlii/Italy/206679-3/2010	ORF3	1.40E-02	109-121	128-140	CWIYNFEGCWCCR
13	AAZ67053.1	Bat SARS CoV Rp3/2004	ORF3	1.00E-05	108-121	121-134	CRWIMRCWGCWKCR
14	ABD75326.1	Bat SARS CoV Rm1/2004	ORF3a	1.30E-05	108-121	121-134	CRWIMRCWGCWKCR
15	ABD75316.1	Bat SARS CoV Rf1/2004	ORF3a	9.8E-05	108-121	121-134	CRWIMRCWGCWKCK
16	AAT76153.1	SARS coronavirus TJF	ORF3	1.60E+00	-	-	-
17	ATN23890.1	Rhinolophus bat coronavirus HKU2	ORF3	4.20E+00	-	-	-
18	AWH65922.1	Pipistrellus bat coronavirus HKU5	ORF3	4.00E+00	-	-	-
19	YP_009328936.1	NL63-related bat coronavirus	ORF3	1.70E-01	-	-	-
20	DX59483.1	Miniopterus bat coronavirus/Kenya/KY27/2006	ORF3	1.30E+00	-	-	-
21	ACA52172.1	Miniopterus bat coronavirus HKU8	ORF3	2.80E+00	-	-	-
22	AVN89325.1	MERs coronavirus	ORF3	2.50E-01	-	-	-
23	AFO70498.1	Human coronavirus NL63	ORF3	2.50E-01	-	-	-
24	AHY21470.1	Human betacoronavirus 2c Jordan-N3/2012	ORF3	8.30E-02	-	-	-
25	ADX59467.1	Eidolon bat coronavirus/Kenya/KY24/2006	ORF3	2.60E+00	-	-	-
26	YP_009380522.1	Coronavirus AcCoV-JC34	ORF3	3.90E+00	-	-	-
27	ADX59459.1	Chaerephon bat coronavirus/Kenya/KY41/2006	ORF3	2.60E+00	-	-	-
28	ADX59452.1	Cardioderma bat coronavirus/Kenya/KY43/2006	ORF3	1.40E+00	-	-	-
29	ACA52158.1	Bat coronavirus 1B	ORF3	9.90E-01	-	-	-
30	YP_001718606.1	Bat coronavirus 1A	ORF3	2.10E-01	-	-	-
31	QBP43280.1	Bat coronavirus	ORF3a	7.80E-01	-	-	-

3.5 Heme linked and Electronic transmission motif of envelope

It was found that the envelope have domains similar to heme linked sites with the same methods of ORF3a protein, respectively. The conserved domain of the envelope is "CWQCCN" (Figure 5.A), E-value=1.1e-2<0.05, which is featured with certain statistical significance. The position of AGG15137.1 is 117-122 (Figure 5.B), and the sequence fragment is "CWQCHS". The position at the envelope is 40-45 (Figure 5.C), and the sequence fragment is "CAYCCN". Through the above analysis, it can be seen that the first two Cys40,Cys43 on this domain are connected to the carbon at the left end of the alpha position and the beta position, respectively, and the last Cys44 is related to the iron of the heme.

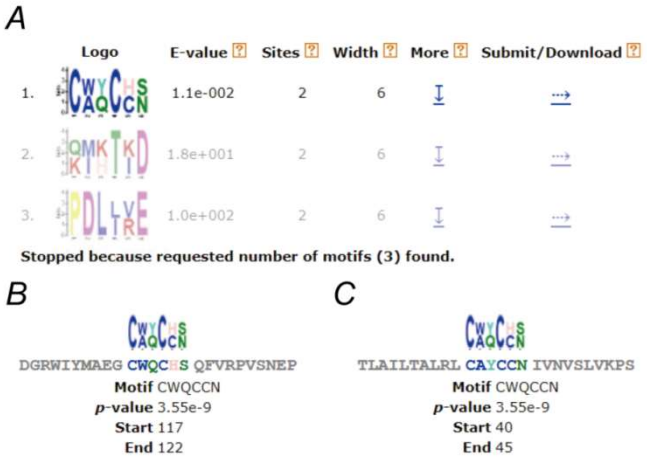

Figure 5. Heme motif of Envelope. ***A***. Heme-linkeddomain"CWQCCN". *B*. heme linked sites at positions 117-122 of AGG15137.1. *C*. heme linked sites at positions 40-45 of Envelope.

Besides, the MEME tool was used to compare the envelope with cytochrome d oxidases (AGH93087.1 cytochrome d oxidase cyd, subunit II [Hydrogenobaculum sp. SN]). Then, it was found that the envelope has a conserved domain (Figure 6), which does not overlap with the heme linked site.The conserved domain of the envelope is "WRHTFD" (Figure 6.A), E-value=2.7e-002<0.05, which is featured with certain statistical significance. The position of AGH93087.1 is 118-123 (Figure 6.B), and the sequence fragment is "WRHTFD". The position at the envelope is 80-85 (Figure 6.C), and the sequence fragment is "QIHTID".

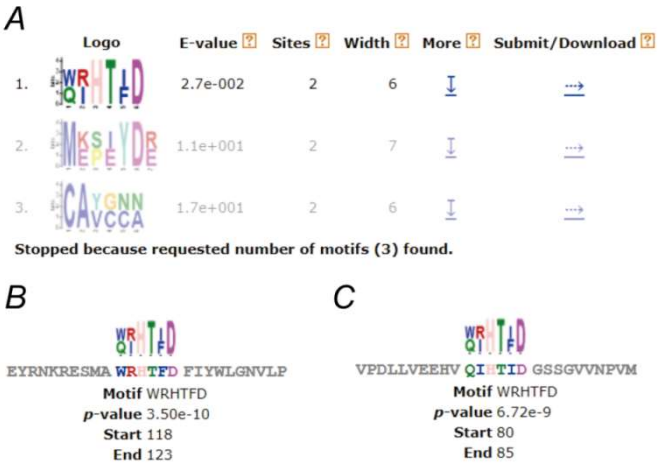

Figure 6. Electronic transmission motif of Envelope. ***A***. Electronic transmissiondomain"WRHTFD". *B*. Electronic transmission sites at positions 118-123 of AGG15137.1. *C*. Electronic transmission sites at positions 80-85 of Envelope.

However, further domain analysis showed that the envelope did not have similar conserved domains as human cytochrome C oxidases (AGW78696.1). It may be that the electron transmission of the envelope is special. Further domain analysis also showed that the envelope did not have a conserved domain similar to Dechelatase (A0A4Y9TPJ9) of Pseudomonas fluorescens. It is probable that the envelope cannot dissociate the iron from the heme at all.

3.6 ORF3a protein catalyzes the dissociation of iron from heme

Researchers found EFeB protein (a type of dechelatase) in bacteria (such as E. coli). The conserved domain of EFeB dissociates the iron in the heme by means of heme oxidases, while the porphyrin ring remains intact. It also has the ability of cytochrome reductases to achieve electron transfer. Pseudomonas fluorescens is a bacterium that can multiply in the blood and release endotoxins, which can cause respiratory infections, sepsis or shock in animals. In addition to that, the MEME tool was used to compare ORF3a with Pseudomonas fluorescens dechelase (tr | A0A4Y9TPJ9 | A0A4Y9TPJ9_PSEFL dechelatase/peroxidase OS = Pseudomonas fluorescens OX = 294 GN = efeB PE = 3 SV = 1). Then, we obtained the conservative domain "IJRRPWNCWKCRNKNGQLDDGNLFJCWQADCEDGCI", E-value = 1.3e-2 <0.05 (Figure 7.A), with certain statistical significance. The position of dechelatase is 347-382(Figure 7.B), which belongs to the conserved domain of EFeB(Figure 7.C, Screenshot from Interpro website). The ORF3a site is 123-158(Figure 7.D), including the conserved domains both in contact with the heme and in electron transport. Cys130, Cys133 and Arg134 are still EFeB conserved domains. If the conserved domain of electron transport is excluded from that of EFeB of ORF3a, only IIe is retained at both ends. IIe at both ends may play an important role in the dissociation of iron from the heme. Since the mechanism of EFeB is still a mystery, molecular simulation technology can't be adopted to simulate the mechanism of iron dissociation from the heme.

We could not fully simulate the dissociation process of iron from heme. Through molecular simulation of DS, we directly connected Cys130, Cys133 and Arg134 of ORF3a to the corresponding positions of heme, and performed "minimization". The two N bonds connected to Fe were automatically broken, but the other two N bonds were not broken. At present, the mechanism of EFeB is not completely clear. We made many attempts and did not know how to break the other two N bonds and keep the porphyrin ring intact.

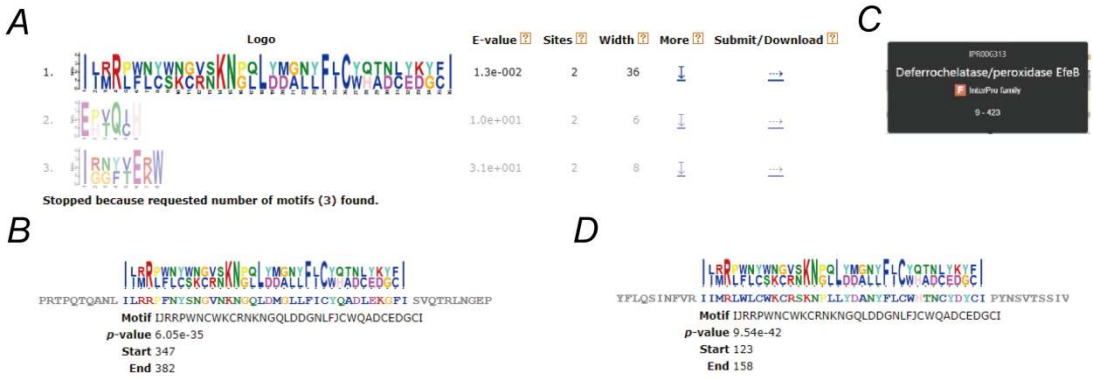

Figure 7. EFeB motif of ORF3a. ***A***. EFeBdomain"IJRRPWNCWKCRNKNGQLDDGNLFJCWQADCEDGCI". ***B***. EFeB domain of A0A4Y9TPJ9. ***C***. EFeB domain sites at positions 347-382 of A0A4Y9TPJ9. ***D***. EFeB domain sites at positions 123-158 of ORF3a.

3.7 ORF3a and ORF8 protein attack the 1-beta chain of the hemoglobin

Iron porphyrin, or heme, is the main porphyrin in the human body. Many hemes are not free but bound to hemoglobin. The novel coronavirus may attack hemoglobin, target heme, and obtain porphyrin. Many viral proteins have domains that bind external and intracellular hemoglobin. It suggests that these viral proteins can assault hemoglobin and cause heme to fall off. ORF3a has two types of motifs: one for binding hemoglobin and the other for heme dissociation. The crystal structures of ORF3a and ORF8 from the SARS-COV-2 virus have been determined. Both of these proteins can form dimers and create pores in the cell membrane. ORF3a also forms tetramers, which may help other viral proteins enter red blood cells more efficiently. We utilized Robetta to model ORF3a and ORF8 to acquire the crystal structures of the complete sequences because the current crystal structures truncated part of the sequences. ORF3a and ORF8 modeling results have a similar 3D structure to the observed primary structure. Robetta cannot be utilized for modeling S protein because the length of the sequence exceeds the 1000-nt restriction. Other viral proteins' modeling results are challenging to comprehend. As a result, only the ORF3a and ORF8 modeling files were used. The aggressive behavior of ORF3a and ORF8 proteins are studied using ZDOCK molecular docking technology. We studied how viral proteins interacted with hemoglobin and discovered the approximate sites of these two proteins on hemoglobin.

The schematic diagram of ORF3a targeting hemoglobin is shown in Figure 8. Figure 8.A shows that the ORF3a monomer is embedded in the 1-beta chain of deoxyhemoglobin. The beta chain's heme is perfectly lodged on ORF3a's heme motif in Figure 8.B. ORF3a's N-terminal segment coincides with the heme of the 1-alpha chain. ORF3a not only assaults hemoglobin but also collects heme. Figure 8.C demonstrates that the ORF3a monomer has no intercalation to oxidized hemoglobin. The heme in Figure 8.D is not incorporated in ORF3a's heme motif. It was noticed that ORF3a's heme motif is also found in the NEAT A, hemoglobin binding region of ORF3a.

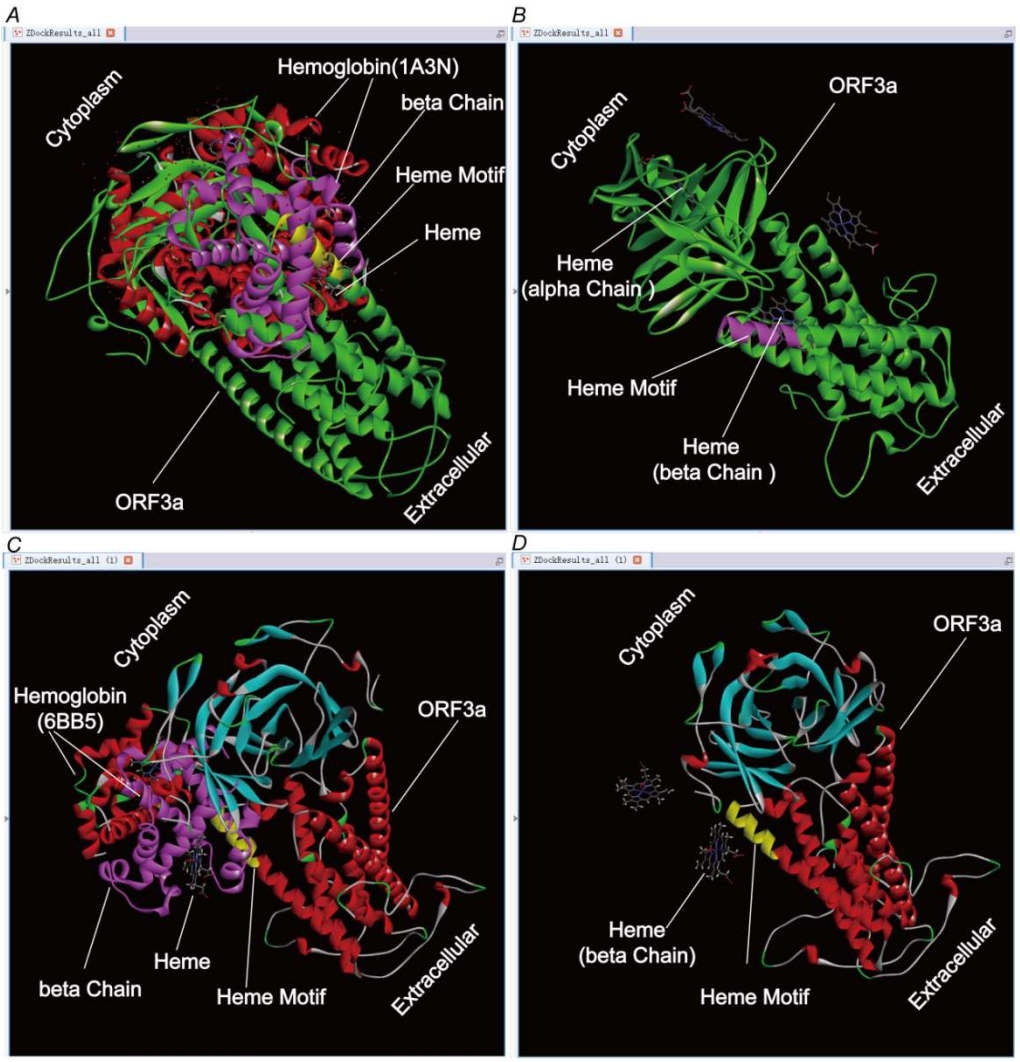

Figure 8. ORF3a protein attacks hemoglobin. ORF3a is a dimer. ***A-B***. ORF3a attacks deoxyhemoglobin. ***C-D***. ORF3a attacks the oxidized hemoglobin. Figures B and D shield the hemoglobin chain and only show hemoglobin.

Figure 9 depicts ORF8 attack hemoglobin. The ORF8 monomer is embedded in the 1-beta chain of deoxyhemoglobin, as shown in Figure 9.A. ORF8's NEAT A hemoglobin binding domain has just been inserted into the 1-beta chain. Figure 9.B indicates that the ORF8 monomer has no intercalation to oxidized hemoglobin.

As viral proteins assault hemoglobin, there will be less and less hemoglobin available to deliver oxygen. Deoxyhemoglobin is more fragile than oxidized hemoglobin, according to the above molecular docking results. As viral proteins infiltrate deoxygenated hemoglobin, the hemoglobin transports carbon dioxide, and blood sugar becomes less and less. Diabetic patients' blood sugar levels may be unstable. Excessive iron, carbon dioxide, and reactive oxygen species (ROS) may cause significant inflammation in the body's cells. Respiratory distress will worsen, causing organs and tissues all over the body to be harmed to varying degrees.

We had identified the viral protein regions that bound hemoglobin. Nevertheless, we could not precisely define the cooperative link between viral proteins due to the limit of the computation tools. ORF3a only had the NEAT domain and no Eryth_link_C domain. So it attacked hemoglobin in red blood cells, not outside the cells. Viral proteins with the Eryth_link_C domain assaulted

hemoglobin outside cells. The viral protein with the NEAT domain attacked hemoglobin in the red blood cell. Even if the red blood cells were hemolyzed to release hemoglobin, the viral protein would damage the hemoglobin causing heme to come off. Furthermore, several viral proteins could bind hemoglobin and disturb its' assemble, which was a virus's insurance strategy. Heme is shed from hemoglobin as a result of this. Viral proteins could bind heme, but only ORF3a and E proteins with more stability binding. ORF3a is bound to heme with the primary goal of dissociating heme into iron and porphyrin. The viral protein captured the porphyrin to obtain membrane penetrability. The E protein was a structural protein that played a role. Heme could take part in a variety of redox processes. The virus bound to heme through the E protein in a stable manner, and the appropriate redox ability was obtained.

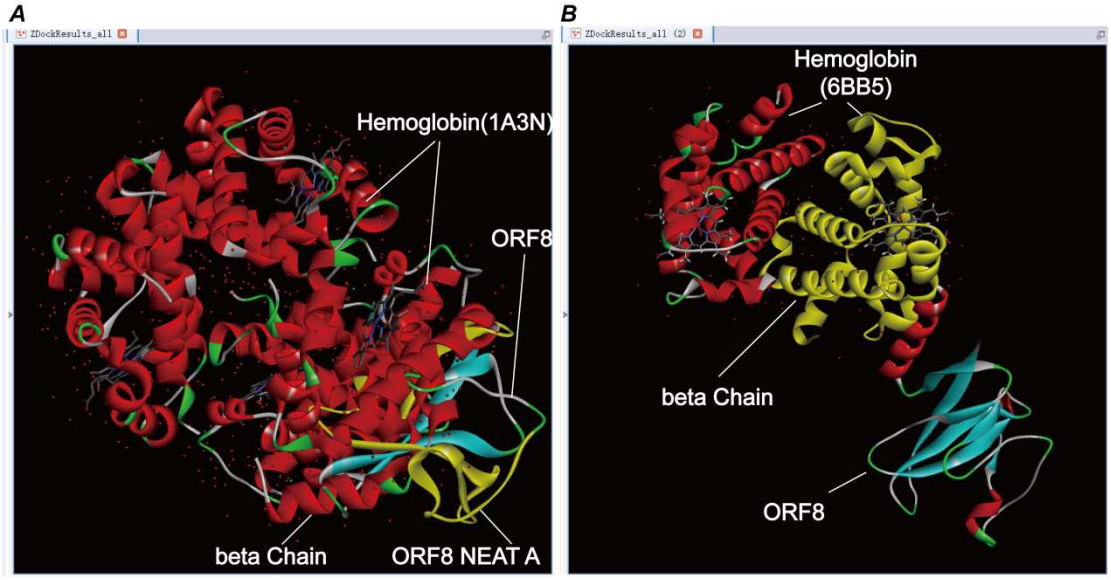

Figure 9. ORF8 protein attacks hemoglobin. ***A***. ORF8 attacks deoxyhemoglobin. ***B***. ORF8 attacks the oxidized hemoglobin.

Control analysis of ORF3a protein attack specificity. ORF3a is a crucial protein that aids in the attack on hemoglobin and the dissociation of hemoglobin. We docked catalase, cytochrome oxidase, myoglobin, and hemocyanin with ORF3a to investigate the specificity of the ORF3a attack (Table 10 and Figure 10). ORF3a protein also assaults cytochrome C mutants, cytochrome P450 mutants, myoglobin mutants, and hemocyanin, as shown in Table 10 and Figure 10. Cytochrome C is a cytochrome oxidase, the only peripheral protein in the outer mitochondrial membrane's electron transport chain. Cardiomyocytes have a higher concentration of cytochrome C. Cytochrome C is involved in transfering electrons to oxygen and plays a crucial role in cell respiration. The attack of cytochrome C G41S results in hypoxia, poisoning of tissue cells, and a reduction in energy metabolism. Cytochrome P450 is implicated in cytokine and body temperature control. Mitochondrial failure, cell death, and Parkinson's syndrome are all possible outcomes of its abnormal function. Myoglobin is solely found in the heart and skeletal muscle; it is not found in other tissues, including smooth muscle. Heart disease and motor system abnormalities can be caused by abnormal myoglobin function. Hemocyanin is a naturally occurring blue respiratory pigment found in the hemolymph of mollusks and arthropods (spiders and beetles).

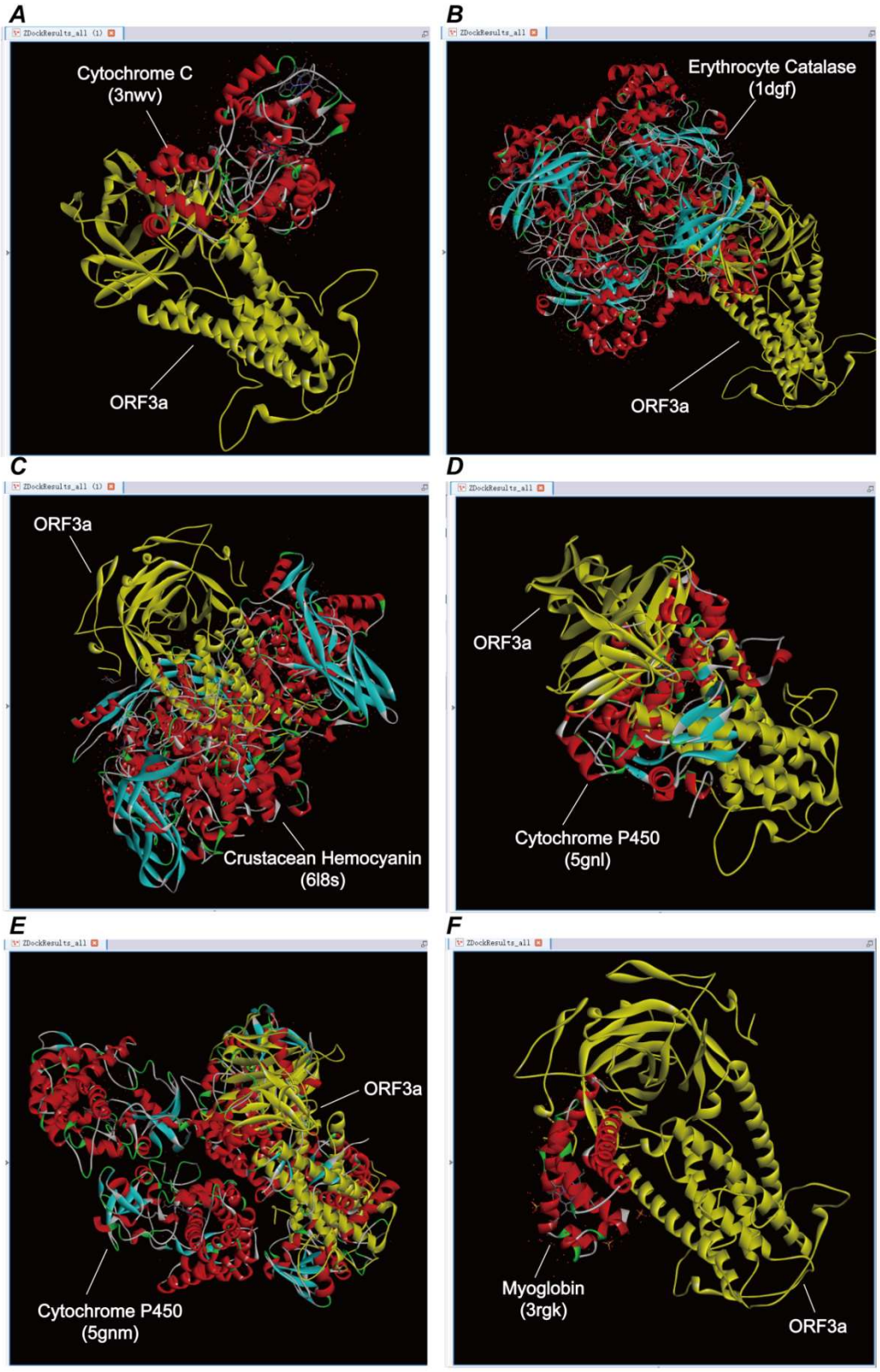

Figure 10. ORF3a attacks other proteins. ***A.*** ORF3a embedded in Human cytochrome C G41S(3nwv). ***B.*** ORF3a embedded in Human erythrocyte catalase (1dgf). ***C.*** ORF3a embedded in crustacean hemocyanin(6l8s). ***D.*** Cytochrome P450 Vdh (CYP107BR1) F106V mutant(5gnl). ***E.*** ORF3a embedded in Cytochrome P450 Vdh (CYP107BR1) L348M mutant(5gnm). ***F.*** ORF3a embedded in Crystal Structure of Human Myoglobin Mutant K45R (3rgk).

Table 10. Docking results between ORF3a and metal porphyrin proteins

No.	Name	Portein	Embed
1	3nwv	Human cytochrome C G41S	Yes
2	5z62	Human cytochrome C	No
3	1dgf	Human erythrocyte catalase	Yes
4	1umk	Human Erythrocyte NADH-cytochrome b5 Reductase	No
5	1w0g	Human cytochrome P450 3A4	No
6	1OG5	P450 CYP2C9	No
7	1v4w	Deoxygenated form of bluefin tuna hemoglobin	No
8	3qjo	Functional unit (KLH1-H) of keyhole limpet hemocyanin	No
9	1lla	Deoxygenated limulus polyphemus subunit II hemocyanin	No
10	1nol	Oxygenated hemocyanin (subunit type ii)	No
11	1js8	Octopus Hemocyanin Functional Unit	No
12	1lnl	deoxygenated hemocyanin from Rapana thomasiana	No
13	6l8s	High-resolution crystal structure of crustacean hemocyanin	Yes
14	5gnl	Cytochrome P450 Vdh (CYP107BR1) F106V mutant	Yes
15	5gnm	Cytochrome P450 Vdh (CYP107BR1) L348M mutant	Yes
16	3rgk	Crystal Structure of Human Myoglobin Mutant K45R	Yes

ORF3a plays an essential role in attacking hemoglobin, which may be specific. In other words, the existing calculation model is based on the docking results of the earlier ORF3a sequence (without considering variation) and the standard hemoglobin structure. If the structure of ORF3a or hemoglobin changes, it may get uncertain results: either hemoglobin is more likely to be attacked; or hemoglobin is less likely to be attacked.

4 Discussion

4.1 Obtaining conserved domains to dissociate iron from the hemethrough gene recombination

For the most primitivelife viruses, it is not so easy to see their role in binding the porphyrin, an ancient compound that widely exists on the earth. It should be noticed that the porphyrin was first found in crude oil and asphalt rock in 1934, and it has unique photoelectronic properties, excellent thermal stability and broad application prospects in materials chemistry, medicine, biochemistry, and analytical chemistry. It is also featured with excellent performance in two-photon absorption, fluorescence effect, energy transfer, and other aspects. Of course, the porphyrin compounds are widely present in photosynthetic or non-photosynthetic organisms, and they are associated with critical physiological processes such as catalysis, oxygen transfer, and energy transfer.Fluorescence resonance energy transfer (FRET) is a non-radiative process in which a donor in an excited state transfers energy to a receptor in the ground state through a long-range

dipole effect. The FRET characteristics of the porphyrin may be the primary survival mode on which the original virus relied.

There are numerous theories about the origin of viruses, one of which is called co-evolution theory, which viruses can evolve from complexes of the protein and the nucleic acid. Various methods do not explain that a virus survived independently of non-appearing cells at the beginning of life, so the origin of a virus remains a mystery. This paper proposes that a virus could be bind to the porphyrin, which could explain the survival problem of an original virus. Because the porphyrin has the energy transfer characteristic of fluorescence resonance, viruses that bind to porphyrins could obtain energy through this light-induced method. A virus that gained power could achieve minimal displacement movements. Depending on the research results in this study, the novel coronavirus was a life form dependent on the porphyrin. Therefore, it was concluded that the novel coronavirus originated from an ancient virus that evolved over countless generations in bats.

This study discovered the heme linked sites of the ORF3a protein belonging to the SARS coronavirus. It was also indirectly confirmed that the novel coronavirus originated from an ancient virus. As we all know, Hydrogenobaculum was acidophilic bacteria in hot springs of karst caves. The overflowing hot spring water formed a river in the cave, which was the water source of various creatures in the cave. There are burrowing animals in the cave, such as civet cats and pangolins. Bats hang upside down, and mainly feed on mosquitoes, while bat feces accumulate on the ground, ferment and acidify.

There may be an ancient virus that obtained the heme linked sites of cytochrome C oxidoreductases in Hydrogenobaculum through genetic recombination. The ancient recombinant virus was released from Hydrogenobaculum and attached to the bat food. Then, bats eat food and are infected with the viruses. It should be noted that there are many viruses in bats. Through the genetic recombination of bats, the ORF3 protein of the coronavirus in the bat gained the heme linked sites on the ancient virus, cytochromereductases and EFeB domains. In this way, coronaviruses evolved into SARS coronaviruses in bats whose feces with the SARS coronavirus also contaminated the environment of other burrowing animals, such as civet cats and pangolins. Then, the civet cats and pangolins infected withthe SARS coronavirus polluted humans' living environment. In this way, humans were infected with the SARS coronavirus. The novel coronavirus SARS-CoV-2 is also a SARS coronavirus, and it may be a new breed of reorganization and evolution in bats.

4.2 S and E protein bind porphyrin to cause high viral infection

The furtherevolution of the novel coronavirus also displays some paradoxical characteristics. The current theory reveals that the novel coronavirus binds to the human ACE2 receptor through a spike protein. The novel coronavirus enters human cells in the form of phagocytosis. The novel coronavirus pneumonia is highly contagious. What causes the high infectivity of the novel coronavirus? The structural proteins S, M, E, and N have the production and binding domains of porphyrin, according to the research.We believe that in addition to the invasive method of spike-ACE2, it should maintain the original invasive pattern. Medical workers have detected the novel coronavirus from urine, saliva, feces, and blood sincethe virus can live in body fluids. In such media, the porphyrin is a prevalent substance, and porphyrin compounds are a class of nitrogen-containing polymers.Existing studies have shown that they have a strong ability to locate and penetrate cell membranes. Therefore, the novel coronavirus may also directly penetrate the

human cell membrane through linking porphyrin.

4.3 Higher hemoglobin causes higher morbidity

The novel coronavirus pneumonia might be closely related to abnormal hemoglobin metabolism in humans. The number of hemoglobin is a significant blood biochemical indicator, and the content varies with genders. The number of normal men is significantly higher than that of normal women, which might also be a reason why men are more likely to be infected with the novel coronavirus pneumonia than women. Besides, most patients with the novel coronavirus pneumonia are themiddle-aged and older adults, whilemany of these patients have underlying diseases such as diabetes. Diabetic patients have higher glycated hemoglobin which is deoxyhemoglobin and is also a combination of hemoglobin and blood glucose, which is another reason for the high infection rate for the elder people. This present study has confirmed that ORF3a could coordinately attack the heme on the beta chain of hemoglobin. Both oxygenated hemoglobin and deoxygenated hemoglobin are attacked, but the latter is more attacked by the virus. During the attack, the positions of ORF3a are slightly different, which shows that the higher the hemoglobin content, the higher the risk of disease. However, it is not sure that the disease rate incited by abnormal hemoglobin (structural) is relatively low. The hemoglobin of patients and rehabilitees could be detected for further research and treatment.

4.4 Interfering with the normal heme anabolic pathway

This article held that the virus directly interfered with the assembly of human hemoglobin. The main reason was that the normal heme was too low. Heme joins in critical biological activities such as regulation of gene expression and protein translation, and the porphyrin is an essential material for the synthesis of the heme. As the existing traces show there is too much free iron in the body of critically ill patients, it could be that the virus-producing molecule competes with iron for the porphyrin, inhibiting the heme anabolic pathway and causing symptoms in humans. It is not clear whether the spatial molecular structure of the heme and porphyrins in patients with porphyria is the same as that in healthy people. If there is an abnormal structure, it is unobvious whether this porphyrin can bind to a viral protein to form a complex, or whether a viral protein can attack this heme. It could be proved by clinical and experimental research.

4.5 Novel coronavirus has a strong carcinogenicity

Numerous published studies demonstrate that after cancer patients get COVID-19, their overall risk of cancer deterioration increases. Numerous clinical studies have established that COVID-19 patients exhibit symptoms consistent with oxidative stress damage. Under conditions of severe oxidative stress, the patient's ROS control mechanism becomes disorganized. The dysregulation of reactive oxygen species (ROS) is a critical element in carcinogenesis. The lungs of the deceased from COVID-19 were mucus-filled, and the deteriorated lung tissue resembled adenocarcinoma-like alterations. We discovered that proteins such as S have a melanoma domain during our search for antigen and membrane fusion domains. Many malignancies, including lung cancer, have pathogenic proteins that contain melanoma domains. Besides, we were conducting computer research and discovered that proteins such as S contain p53 domains. Normal cells could develop cancer cells when the P53 protein was mutated. We believe that the SARS-COV-2 virus is highly carcinogenic based on these comprehensive characteristics.

5. Conclusion

Since the outbreak of the epidemic, it is of great scientific significance to use bioinformatics to analyze novel coronavirus proteins' roles. In this study, conserved domain analysis, homology modeling, and molecular docking was made to compare the biological functions of specific proteins belonging to the novel coronavirus.

A conserved domain search strategy was utilized in this present study to determine that a large number of viral proteins could bind to hemoglobin. S could bind to extracellular hemoglobin. Viral proteins interacted with porphyrins and worked together to produce heme. Both E and ORF3a contained heme-binding sites. ORF3a's Arg134 and E's Cys44 were the heme-iron binding sites, respectively. ORF3a also contained homologous domains to human cytochrome C reductase and bacterial EFeB protein. So ORF3a was capable of decomposing heme into iron and porphyrin. The molecular docking analysis revealed that ORF3a and ORF8 proteins could attack hemoglobin's 1-beta chain and capture the heme. Deoxyhemoglobin was more susceptible to viral attack than oxidized hemoglobin. Besides, ORF3a could bind hemocyanin, cytochrome, peroxidase, and myoglobin. But it is not clear whether the immune and blood systems of blue blood organisms can resist the new coronavirus.

In short, the SARS-COV-2 virus is carcinogenic. The combination of viral proteins to porphyrins and their metal compounds would improve the unmatched ability to permeate cell membranes and generate oxygen free radicals (ROS). It may be associated with viral infections and epidemic transmission. Viral proteins regulated the production and function of NO, CO and CO2 by inhibiting the activity of hemoglobin, thereby affecting immune cell function. Viral proteins' attack on hemoglobin could result in symptoms such as respiratory distress and blood clotting, damage to numerous organs and tissues, and disruption of normal human heme metabolism.

Declarations

Ethics approval and consent to participate

Not applicable.

Consent for publication

Not applicable.

Availability of data and material

The datasets and results supporting the conclusions of this article are available at https://pan.baidu.com/s/1wMnj_kquhXPmXsT5Cz3j4g, code: iare.
Or: https://mega.nz/folder/M3YRlapI#BAdg4zeQ7nocr_eXSl1sTA

Competing interests

The authors declare that they have no competing interests.

Funding

This work was funded by a grant from the Talent Introduction Project of Sichuan University of Science and Engineering (award number: 2018RCL20, grant recipient: WZL).

Author's contribution

Funding was obtained by WZL. Besides, design, analysis and writing are finished by WZL, while data curation and manuscript check are undertaken by HLL. Both authors have read and agreed to the published version of the manuscript.

Acknowledgements

Not applicable.

Author details

[1] School of Computer Science and Engineering, Sichuan University of Science & Engineering, Zigong, 643002, China.
[2] School of Life Science and Food Engineering, Yibin University, Yibin, 644000, China.

References

1. Diao, K., P. Han, T. Pang, Y. Li, and Z. Yang. 2020. HRCT Imaging Features in Representative Imported Cases of 2019 Novel Coronavirus Pneumonia. *Precision Clinical Medicine*.
2. Chang, D., M. Lin, L. Wei, L. Xie, G. Zhu, C. S. D. Cruz, and L. Sharma. 2020. Epidemiologic and clinical characteristics of novel coronavirus infections involving 13 patients outside Wuhan, China. *JAMA*.
3. Huang, C., Y. Wang, X. Li, L. Ren, J. Zhao, Y. Hu, L. Zhang, G. Fan, J. Xu, and X. Gu. 2020. Clinical features of patients infected with 2019 novel coronavirus in Wuhan, China. *The Lancet*.
4. Song, Y., P. Liu, X. Shi, Y. Chu, J. Zhang, J. Xia, X. Gao, T. Qu, and M. Wang. 2020. SARS-CoV-2 induced diarrhoea as onset symptom in patient with COVID-19. *Gut*.
5. Yao, X., T. Li, Z. He, Y. Ping, H. Liu, S. Yu, H. Mou, L. Wang, H. Zhang, and W. Fu. 2020. A pathological report of three COVID-19 cases by minimally invasive autopsies. *Zhonghua bing li xue za zhi= Chinese journal of pathology* 49: E009-E009.
6. Dolhnikoff, M., A. N. Duarte-Neto, R. A. de Almeida Monteiro, L. F. Ferraz da Silva, E. Pierre de Oliveira, P. H. Nascimento Saldiva, T. Mauad, and E. Marcia Negri. 2020. Pathological evidence of pulmonary thrombotic phenomena in severe COVID-19. *Journal of Thrombosis and Haemostasis*.
7. Zhu, N., D. Zhang, W. Wang, X. Li, B. Yang, J. Song, X. Zhao, B. Huang, W. Shi, and R. Lu. 2020. A novel coronavirus from patients with pneumonia in China, 2019. *New England Journal of Medicine*.
8. Wu, F., S. Zhao, B. Yu, Y.-M. Chen, W. Wang, Z.-G. Song, Y. Hu, Z.-W. Tao, J.-H. Tian, and Y.-Y. Pei. 2020. A new coronavirus associated with human respiratory disease in China. *Nature*: 1-8.
9. Lu, H., C. W. Stratton, and Y. W. Tang. Outbreak of Pneumonia of Unknown Etiology in Wuhan China: the Mystery and the Miracle. *Journal of Medical Virology*.
10. Zhu, N., D. Zhang, W. Wang, X. Li, B. Yang, J. Song, X. Zhao, B. Huang, W. Shi, and R. Lu. 2020. China Novel Coronavirus Investigating and Research Team. A novel coronavirus from patients with pneumonia in China, 2019. *N Engl J Med*.
11. Lu, R., X. Zhao, J. Li, P. Niu, B. Yang, H. Wu, W. Wang, H. Song, B. Huang, and N. Zhu. 2020. Genomic characterisation and epidemiology of 2019 novel coronavirus: implications for virus origins and receptor binding. *The Lancet*.
12. Wang, M., Y. Zhou, Z. Zong, Z. Liang, Y. Cao, H. Tang, B. Song, Z. Huang, Y. Kang, and P. Feng. 2020. A precision medicine approach to managing Wuhan Coronavirus pneumonia. *Precision Clinical Medicine*.
13. Schaecher, S. R., and A. Pekosz. 2010. SARS coronavirus accessory gene expression and function. In *Molecular Biology of the SARS-Coronavirus*. Springer. 153-166.

14. McBride, R., and B. C. Fielding. 2012. The role of severe acute respiratory syndrome (SARS)-coronavirus accessory proteins in virus pathogenesis. *Viruses* 4: 2902-2923.
15. Wu, A., Y. Peng, B. Huang, X. Ding, X. Wang, P. Niu, J. Meng, Z. Zhu, Z. Zhang, and J. Wang. 2020. Genome Composition and Divergence of the Novel Coronavirus (2019-nCoV) Originating in China. *Cell Host & Microbe*.
16. Paraskevis, D., E. G. Kostaki, G. Magiorkinis, G. Panayiotakopoulos, G. Sourvinos, and S. Tsiodras. 2020. Full-genome evolutionary analysis of the novel corona virus (2019-nCoV) rejects the hypothesis of emergence as a result of a recent recombination event. *Infection, Genetics and Evolution*: 104212.
17. Li, S., L. Yuan, G. Dai, R. A. Chen, D. X. Liu, and T. S. Fung. 2020. Regulation of the ER Stress Response by the Ion Channel Activity of the Infectious Bronchitis Coronavirus Envelope Protein Modulates Virion Release, Apoptosis, Viral Fitness, and Pathogenesis. *Frontiers in Microbiology* 10: 3022.
18. To, K. K.-W., O. T. Y. Tsang, C. Chik-Yan Yip, K.-H. Chan, T.-C. Wu, J. Chan, W.-S. Leung, T. S.-H. Chik, C. Y.-C. Choi, and D. H. Kandamby. 2020. Consistent detection of 2019 novel coronavirus in saliva. *Clinical Infectious Diseases*.
19. Rothe, C., M. Schunk, P. Sothmann, G. Bretzel, G. Froeschl, C. Wallrauch, T. Zimmer, V. Thiel, C. Janke, and W. Guggemos. 2020. Transmission of 2019-nCoV infection from an asymptomatic contact in Germany. *New England Journal of Medicine*.
20. Chen, N., M. Zhou, X. Dong, J. Qu, F. Gong, Y. Han, Y. Qiu, J. Wang, Y. Liu, and Y. Wei. 2020. Epidemiological and clinical characteristics of 99 cases of 2019 novel coronavirus pneumonia in Wuhan, China: a descriptive study. *The Lancet*.
21. Quaye, I. K. 2015. Extracellular hemoglobin: the case of a friend turned foe. *Frontiers in physiology* 6: 96-96.
22. Das, R., and P. Sharma. 2020. Disorders of abnormal hemoglobin. In *Clinical Molecular Medicine*. Elsevier. 327-339.
23. Kazazian Jr, H. H., and A. P. Woodhead. 1973. Hemoglobin A synthesis in the developing fetus. *New England Journal of Medicine* 289: 58-62.
24. Pan, F., T. Ye, P. Sun, S. Gui, B. Liang, L. Li, D. Zheng, J. Wang, R. L. Hesketh, and L. Yang. 2020. Time course of lung changes on chest CT during recovery from 2019 novel coronavirus (COVID-19) pneumonia. *Radiology*: 200370.
25. Poggiali, E., A. Dacrema, D. Bastoni, V. Tinelli, E. Demichele, P. Mateo Ramos, T. Marcianò, M. Silva, A. Vercelli, and A. Magnacavallo. 2020. Can lung US help critical care clinicians in the early diagnosis of novel coronavirus (COVID-19) Pneumonia? *Radiology*: 200847.
26. Lei, J., J. Li, X. Li, and X. Qi. 2020. CT imaging of the 2019 novel coronavirus (2019-nCoV) pneumonia. *Radiology* 295: 18-18.
27. Hong, X., J. Xiong, Z. Feng, and Y. Shi. 2020. Extracorporeal membrane oxygenation (ECMO): does it have a role in the treatment of severe COVID-19? *International Journal of Infectious Diseases*.
28. Ñamendys-Silva, S. A. 2020. ECMO for ARDS due to COVID-19. *Heart & Lung: The Journal of Cardiopulmonary and Acute Care*.
29. Henry, B. M., and G. Lippi. 2020. Poor survival with extracorporeal membrane oxygenation in acute respiratory distress syndrome (ARDS) due to coronavirus disease 2019 (COVID-19): Pooled analysis of early reports. *Journal of Critical Care*.
30. Zhang, W., Y. Zhao, F. Zhang, Q. Wang, T. Li, Z. Liu, J. Wang, Y. Qin, X. Zhang, and X. Yan. 2020. The use of anti-inflammatory drugs in the treatment of people with severe coronavirus disease 2019 (COVID-19): The experience of clinical immunologists from China. *Clinical Immunology*: 108393.

31. McGonagle, D., K. Sharif, A. O'Regan, and C. Bridgewood. 2020. Interleukin-6 use in COVID-19 pneumonia related macrophage activation syndrome. *Autoimmunity reviews*: 102537.
32. Leichtman, D. A., and G. J. Brewer. 1978. Elevated plasma levels of fibrinopeptide A during sickle cell anemia pain crisis–evidence for intravascular coagulation. *American journal of hematology* 5: 183-190.
33. Rojanasthien, S., V. Surakamolleart, S. Boonpucknavig, and P. Isarangkura. 1992. Hematological and coagulation studies in malaria. *Journal of the Medical Association of Thailand= Chotmaihet thangphaet* 75: 190-194.
34. Ogata, T., M. Kamouchi, T. Kitazono, J. Kuroda, H. Ooboshi, T. Shono, T. Morioka, S. Ibayashi, T. Sasaki, and M. Iida. 2008. Cerebral venous thrombosis associated with iron deficiency anemia. *Journal of Stroke and Cerebrovascular Diseases* 17: 426-428.
35. Alder, L., and A. Tambe. 2019. Acute Anemia. In *StatPearls [Internet]*. StatPearls Publishing.
36. Gao, Y., T. Li, M. Han, X. Li, D. Wu, Y. Xu, Y. Zhu, Y. Liu, X. Wang, and L. Wang. 2020. Diagnostic utility of clinical laboratory data determinations for patients with the severe COVID-19. *Journal of Medical Virology*.
37. Tang, N., D. Li, X. Wang, and Z. Sun. 2020. Abnormal coagulation parameters are associated with poor prognosis in patients with novel coronavirus pneumonia. *Journal of Thrombosis and Haemostasis*.
38. Wang, X., W. Xu, G. Hu, S. Xia, Z. Sun, Z. Liu, Y. Xie, R. Zhang, S. Jiang, and L. Lu. 2020. SARS-CoV-2 infects T lymphocytes through its spike protein-mediated membrane fusion. *Cellular & Molecular Immunology*: 1-3.
39. Wang, F., J. Nie, H. Wang, Q. Zhao, Y. Xiong, L. Deng, S. Song, Z. Ma, P. Mo, and Y. Zhang. 2020. Characteristics of peripheral lymphocyte subset alteration in COVID-19 pneumonia. *The Journal of infectious diseases*.
40. Borghetti, A., A. Ciccullo, E. Visconti, E. Tamburrini, and S. Di Giambenedetto. COVID-19 diagnosis does not rule out other concomitant diseases. *European Journal of Clinical Investigation*: e13241.
41. Li, S.-r., Z.-j. Tang, Z.-h. Li, and X. Liu. 2020. Searching therapeutic strategy of new coronavirus pneumonia from angiotensin-converting enzyme 2: the target of COVID-19 and SARS-CoV. *European Journal of Clinical Microbiology & Infectious Diseases*: 1.
42. Luo, W., H. Yu, J. Gou, X. Li, Y. Sun, J. Li, and L. Liu. 2020. Clinical pathology of critical patient with novel coronavirus pneumonia (COVID-19). *Pathology & Pathobiology* 2020020407.
43. Emmons, R., L. Oshiro, H. Johnson, and E. Lennette. 1972. Intra-erythrocytic location of Colorado tick fever virus. *Journal of General Virology* 17: 185-195.
44. Mitra, A., D. M. Dwyre, M. Schivo, G. R. Thompson, S. H. Cohen, N. Ku, and J. P. Graff. 2020. Leukoerythroblastic reaction in a patient with COVID-19 infection. *American Journal of Hematology*.
45. Bhardwaj, K., P. Liu, J. L. Leibowitz, and C. C. Kao. 2012. The coronavirus endoribonuclease Nsp15 interacts with retinoblastoma tumor suppressor protein. *Journal of virology* 86: 4294-4304.
46. Spring, F. A., C. H. Holmes, K. L. Simpson, W. J. Mawby, M. Jules Mattes, Y. Okubo, and S. F. Parsons. 1997. The Oka blood group antigen is a marker for the M6 leukocyte activation antigen, the human homolog of OX-47 antigen, basigin and neurothelin, an immunoglobulin superfamily molecule that is widely expressed in human cells and tissues. *European journal of immunology* 27: 891-897.
47. Szempruch, A. J., S. E. Sykes, R. Kieft, L. Dennison, A. C. Becker, A. Gartrell, W. J. Martin, E. S. Nakayasu, I. C. Almeida, and S. L. Hajduk. 2016. Extracellular vesicles from Trypanosoma brucei mediate virulence factor transfer and cause host anemia. *Cell* 164: 246-257.

48. Howell, S. A., I. Well, S. L. Fleck, C. Kettleborough, C. R. Collins, and M. J. Blackman. 2003. A single malaria merozoite serine protease mediates shedding of multiple surface proteins by juxtamembrane cleavage. *Journal of Biological Chemistry* 278: 23890-23898.
49. Mitchell, G., A. Thomas, G. Margos, A. Dluzewski, and L. Bannister. 2004. Apical membrane antigen 1, a major malaria vaccine candidate, mediates the close attachment of invasive merozoites to host red blood cells. *Infection and immunity* 72: 154-158.
50. Crosnier, C., L. Y. Bustamante, S. J. Bartholdson, A. K. Bei, M. Theron, M. Uchikawa, S. Mboup, O. Ndir, D. P. Kwiatkowski, and M. T. Duraisingh. 2011. Basigin is a receptor essential for erythrocyte invasion by Plasmodium falciparum. *Nature* 480: 534-537.
51. Galatas, B., Q. Bassat, and A. Mayor. 2016. Malaria Parasites in the Asymptomatic: Looking for the Hay in the Haystack. *Trends Parasitol* 32: 296-308.
52. Iesa, M. A., M. E. Osman, M. A. Hassan, A. I. Dirar, N. Abuzeid, J. J. Mancuso, R. Pandey, A. A. Mohammed, M. J. Borad, and H. M. Babiker. 2020. SARS-CoV-2 and Plasmodium falciparum common immunodominant regions may explain low COVID-19 incidence in the malaria-endemic belt. *New microbes and new infections* 38: 100817.
53. Sigala, P. A., and D. E. Goldberg. 2014. The Peculiarities and Paradoxes of Plasmodium Heme Metabolism. *Annual Review of Microbiology* 68: 259-278.
54. Kaluka, D. 2019. Heme-containing proteins in the Malaria Parasite. *Science Semina* 6: https://pillars.taylor.edu/science-seminar/6.
55. Goldberg, D. E., and P. A. Sigala. 2017. Plasmodium heme biosynthesis: To be or not to be essential? *PLoS pathogens* 13: e1006511-e1006511.
56. Nagaraj, V. A., B. Sundaram, N. M. Varadarajan, P. A. Subramani, D. M. Kalappa, S. K. Ghosh, and G. Padmanaban. 2013. Malaria Parasite-Synthesized Heme Is Essential in the Mosquito and Liver Stages and Complements Host Heme in the Blood Stages of Infection. *PLOS Pathogens* 9: e1003522.
57. Matz, J. M., B. Drepper, T. B. Blum, E. van Genderen, A. Burrell, P. Martin, T. Stach, L. M. Collinson, J. P. Abrahams, K. Matuschewski, and M. J. Blackman. 2020. A lipocalin mediates unidirectional heme biomineralization in malaria parasites. *Proceedings of the National Academy of Sciences* 117: 16546-16556.
58. Kapishnikov, S., D. Grolimund, G. Schneider, E. Pereiro, J. G. McNally, J. Als-Nielsen, and L. Leiserowitz. 2017. Unraveling heme detoxification in the malaria parasite by in situ correlative X-ray fluorescence microscopy and soft X-ray tomography. *Scientific Reports* 7: 7610.
59. Abshire, J. R., C. J. Rowlands, S. M. Ganesan, P. T. C. So, and J. C. Niles. 2017. Quantification of labile heme in live malaria parasites using a genetically encoded biosensor. *Proceedings of the National Academy of Sciences* 114: E2068-E2076.
60. Ke, H., P. A. Sigala, K. Miura, J. M. Morrisey, M. W. Mather, J. R. Crowley, J. P. Henderson, D. E. Goldberg, C. A. Long, and A. B. Vaidya. 2014. The heme biosynthesis pathway is essential for Plasmodium falciparum development in mosquito stage but not in blood stages. *Journal of Biological Chemistry* 289: 34827-34837.
61. Bottino-Rojas, V., O. A. Talyuli, N. Jupatanakul, S. Sim, G. Dimopoulos, T. M. Venancio, A. C. Bahia, M. H. Sorgine, P. L. Oliveira, and G. O. Paiva-Silva. 2015. Heme signaling impacts global gene expression, immunity and dengue virus infectivity in Aedes aegypti. *PLoS One* 10: e0135985.
62. Vzorov, A. N., D. W. Dixon, J. S. Trommel, L. G. Marzilli, and R. W. Compans. 2002. Inactivation of human immunodeficiency virus type 1 by porphyrins. *Antimicrob Agents Chemother* 46: 3917-3925.
63. Levere, R. D., Y.-F. Gong, A. Kappas, D. J. Bucher, G. P. Wormser, and N. G. Abraham. 1991. Heme inhibits human immunodeficiency virus 1 replication in cell cultures and enhances the antiviral effect of zidovudine. *Proceedings of the National Academy of Sciences* 88: 1756-1759.

64. Espinoza, J. A., M. A. León, P. F. Céspedes, R. S. Gómez, G. Canedo-Marroquín, S. A. Riquelme, F. J. Salazar-Echegarai, P. Blancou, T. Simon, I. Anegon, M. K. Lay, P. A. González, C. A. Riedel, S. M. Bueno, and A. M. Kalergis. 2017. Heme Oxygenase-1 Modulates Human Respiratory Syncytial Virus Replication and Lung Pathogenesis during Infection. *The Journal of Immunology* 199: 212-223.
65. Espinoza, J. A., and M. A. León. 2017. Heme Oxygenase-1 Modulates Human Respiratory Syncytial Virus Replication and Lung Pathogenesis during Infection. 199: 212-223.
66. El Kalamouni, C., E. Frumence, S. Bos, J. Turpin, B. Nativel, W. Harrabi, D. A. Wilkinson, O. Meilhac, G. Gadea, P. Desprès, P. Krejbich-Trotot, and W. Viranaïcken. 2018. Subversion of the Heme Oxygenase-1 Antiviral Activity by Zika Virus. *Viruses* 11: 2.
67. Gomi, H., K. Hatanaka, T. Miura, and I. Matsuo. 1997. Type of Impaired Porphyrin Metabolism Caused by Hepatitis C Virus Is Not Porphyria Cutanea Tarda but Chronic Hepatic Porphyria. *Archives of Dermatology* 133: 1170-1171.
68. Bernardo-Seisdedos, G., D. Gil, J.-M. Blouin, E. Richard, and O. Millet. 2020. Natural and pharmacological chaperones against accelerated protein degradation: uroporphyrinogen III synthase and congenital erythropoietic porphyria. In *Protein Homeostasis Diseases*. Elsevier. 389-413.
69. Lameda, I. L. P., and T. R. Koch. 2020. Acquired Metabolic Disorders. In *Liver Diseases*. Springer. 107-116.
70. Zhang, H., H. Long, L. Ma, G. Wang, Q.-R. Mu, Y.-P. Ran, Q.-Z. Liu, S.-X. Xiao, X.-J. Zhang, and J.-Z. Zhang. 2020. Consensus on pre-examination and triage in clinic of dermatology during outbreak of COVID-19 from Chinese experts. *International Journal of Dermatology and Venereology*.
71. Recalcati, S. 2020. Cutaneous manifestations in COVID-19: a first perspective. *Journal of the European Academy of Dermatology and Venereology*.
72. Liang, W., Z. Feng, S. Rao, C. Xiao, X. Xue, Z. Lin, Q. Zhang, and W. Qi. 2020. Diarrhoea may be underestimated: a missing link in 2019 novel coronavirus. *Gut*.
73. Chan, J. F.-W., S. Yuan, K.-H. Kok, K. K.-W. To, H. Chu, J. Yang, F. Xing, J. Liu, C. C.-Y. Yip, and R. W.-S. Poon. 2020. A familial cluster of pneumonia associated with the 2019 novel coronavirus indicating person-to-person transmission: a study of a family cluster. *The Lancet* 395: 514-523.
74. Hassan, S., F. N. Sheikh, S. Jamal, J. K. Ezeh, and A. Akhtar. 2020. Coronavirus (COVID-19): a review of clinical features, diagnosis, and treatment. *Cureus* 12.
75. Lippi, G., A. M. South, and B. M. Henry. 2020. ANNALS EXPRESS: Electrolyte Imbalances in Patients with Severe Coronavirus Disease 2019 (COVID-19). *Annals of Clinical Biochemistry*: 0004563220922255.
76. Xiong, T.-Y., S. Redwood, B. Prendergast, and M. Chen. 2020. Coronaviruses and the cardiovascular system: acute and long-term implications. *European Heart Journal*.
77. Zhang, C., L. Shi, and F.-S. Wang. 2020. Liver injury in COVID-19: management and challenges. *The Lancet Gastroenterology & Hepatology*.
78. Naicker, S., C.-W. Yang, S.-J. Hwang, B.-C. Liu, J.-H. Chen, and V. Jha. 2020. The Novel Coronavirus 2019 epidemic and kidneys. *Kidney International*.
79. Wu, Y., X. Xu, Z. Chen, J. Duan, K. Hashimoto, L. Yang, C. Liu, and C. Yang. 2020. Nervous system involvement after infection with COVID-19 and other coronaviruses. *Brain, Behavior, and Immunity*.
80. Mungroo, M. R., N. A. Khan, and R. Siddiqui. 2020. Novel Coronavirus: Current Understanding of Clinical Features, Diagnosis, Pathogenesis, and Treatment Options. *Pathogens* 9: 297.
81. Lu, L., W. Xiong, D. Liu, J. Liu, D. Yang, N. Li, J. Mu, J. Guo, W. Li, and G. Wang. 2020. New-onset acute symptomatic seizure and risk factors in Corona Virus Disease 2019: A Retrospective Multicenter Study. *Epilepsia*.

82. Wang, H.-Y., X.-L. Li, Z.-R. Yan, X.-P. Sun, J. Han, and B.-W. Zhang. 2020. Potential neurological symptoms of COVID-19. *Therapeutic Advances in Neurological Disorders* 13: 1756286420917830.
83. Moriguchi, T., N. Harii, J. Goto, D. Harada, H. Sugawara, J. Takamino, M. Ueno, H. Sakata, K. Kondo, and N. Myose. 2020. A first case of meningitis/encephalitis associated with SARS-Coronavirus-2. *International Journal of Infectious Diseases*.
84. Liu, K., M. Pan, Z. Xiao, and X. Xu. 2020. Neurological manifestations of the coronavirus (SARS-CoV-2) pandemic 2019–2020. *Journal of Neurology, Neurosurgery & Psychiatry*.
85. Romeo, G., and E. Y. Levin. 1969. Uroporphyrinogen 3 cosynthetase in human congenital erythropoietic porphyria. *Proceedings of the National Academy of Sciences of the United States of America* 63: 856-863.
86. Rabiee, M., N. Rabiee, R. Salarian, and G. Rabiee. 2019. Porphyrin-based nanomaterials. In *Introduction to Nanomaterials in Medicine*. Morgan & Claypool Publishers. 6-1-6-24.
87. Sułek, A., B. Pucelik, M. Kobielusz, A. Barzowska, and J. M. Dąbrowski. 2020. Photodynamic Inactivation of Bacteria with Porphyrin Derivatives: Effect of Charge, Lipophilicity, ROS Generation, and Cellular Uptake on Their Biological Activity In Vitro. *Int J Mol Sci* 21: 8716.
88. Tsubone, T. M., W. K. Martins, C. Pavani, H. C. Junqueira, R. Itri, and M. S. Baptista. 2017. Enhanced efficiency of cell death by lysosome-specific photodamage. 7: 6734.
89. Kolarova, H., P. Nevrelova, K. Tomankova, P. Kolar, R. Bajgar, and J. Mosinger. 2008. Production of reactive oxygen species after photodynamic therapy by porphyrin sensitizers. *General physiology and biophysics* 27: 101-105.
90. Nishida, K., T. Tojo, T. Kondo, and M. Yuasa. 2021. Evaluation of the correlation between porphyrin accumulation in cancer cells and functional positions for application as a drug carrier. *Scientific Reports* 11: 2046.
91. Clichici, S., A. Filip, D. Daicoviciu, R. M. Ion, T. Mocan, C. Tatomir, L. Rogojan, D. Olteanu, and A. Muresan. 2010. The dynamics of reactive oxygen species in photodynamic therapy with tetra sulfophenyl-porphyrin. *Acta physiologica Hungarica* 97: 41-51.
92. Babbitt, S. E., J. Hsu, D. L. Mendez, and R. G. Kranz. 2017. Biosynthesis of single thioether c-type cytochromes provides insight into mechanisms intrinsic to holocytochrome c synthase (HCCS). *Biochemistry* 56: 3337-3346.